Journal of Medicinal Chemistry

Article

pubs.acs.org/jmc

Synthesis and Biological Evaluation of the First Triple Inhibitors of Human Topoisomerase 1, Tyrosyl−DNA Phosphodiesterase 1 (Tdp1), and Tyrosyl−DNA Phosphodiesterase 2 (Tdp2)

Ping Wang,[†] Mohamed S. A. Elsayed,[†] Caroline B. Plescia,[‡] Azhar Ravji,[‡] Christophe E. Redon,[‡] Evgeny Kiselev,[‡] Christophe Marchand,[‡] Olga Zeleznik,[‡] Keli Agama,[‡] Yves Pommier,[‡] and Mark Cushman*[,†]

[†]Department of Medicinal Chemistry and Molecular Pharmacology, College of Pharmacy, and the Purdue Center for Cancer Research, Purdue University, West Lafayette, Indiana 47907, United States

[‡]Developmental Therapeutics Branch and Laboratory of Molecular Pharmacology, Center for Cancer Research, National Institutes of Health, Bethesda, Frederick, Maryland 20892, United States

S *Supporting Information*

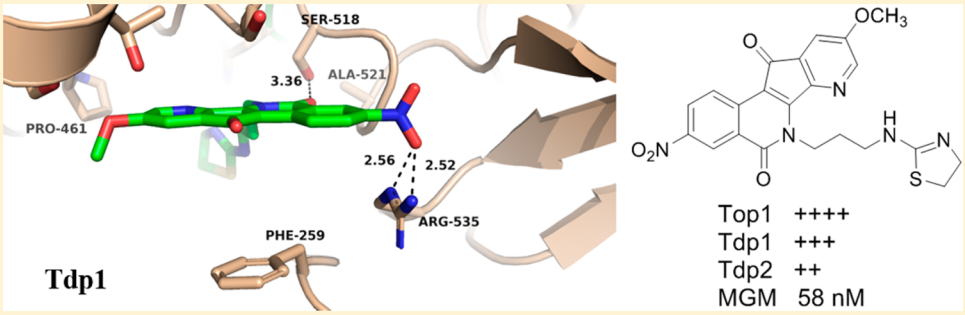

ABSTRACT: Tdp1 and Tdp2 are two tyrosyl−DNA phosphodiesterases that can repair damaged DNA resulting from topoisomerase inhibitors and a variety of other DNA-damaging agents. Both Tdp1 and Tdp2 inhibition could hypothetically potentiate the cytotoxicities of topoisomerase inhibitors. This study reports the successful structure-based design and synthesis of new 7-azaindenoisoquinolines that act as triple inhibitors of Top1, Tdp1, and Tdp2. Enzyme inhibitory data and cytotoxicity data from human cancer cell cultures establish that modification of the lactam side chain of the 7-azaindenoisoquinolines can modulate their inhibitory potencies and selectivities vs Top1, Tdp1, and Tdp2. Molecular modeling of selected target compounds bound to Top1, Tdp1, and Tdp2 was used to design the inhibitors and facilitate the structure−activity relationship analysis. The monitoring of DNA damage by γ-H2AX foci formation in human PBMCs (lymphocytes) and acute lymphoblastic leukemia CCRF-CEM cells documented significantly more DNA damage in the cancer cells vs normal cells.

INTRODUCTION

The inhibition of DNA topoisomerase I (Top1) has proven to be a successful approach to the design of anticancer agents. Camptothecins (CPTs) and indenoisoquinolines are two established classes of Top1 inhibitors.[1,2] The CPTs and indenoisoquinolines act through stabilization of the DNA-Top1 covalent cleavage complex (Top1cc) by a dual DNA intercalation and protein binding mechanism that leads to inhibition of the DNA religation process.[1,3−5] Subsequent collision of the DNA replication fork with drug-stabilized complexes causes DNA double-stranded breaks. Ultimately, this leads to tumor cell death. DNA repair after Top1-mediated DNA cleavage is a complex process that can be initiated by tyrosyl−DNA phosphodiesterase 1 (Tdp1),[6−8] which plays a critical role in development of drug resistance.[9] Tdp1 is a member of the phospholipase D superfamily[10] of enzymes that catalyze the hydrolysis of the 3′-phosphotyrosyl linker found in the Top1cc and other 3′-end DNA blocking lesions.[10−13] The proposed mechanism for Tdp1-mediated hydrolysis involves two sequential steps.[8,10,11] In the first step, a conserved histidine residue His263 performs a nucleophilic attack on the phosphate moiety that is linked to Top1 catalytic residue Tyr723 at the 3′-end of DNA (Figure 1A), releasing tyrosine and forming a covalent enzyme−DNA complex (Figure 1B), while in the second step the intermediate phosphohistidine complex is hydrolyzed via nucleophilic attack by a His493-activated water molecule (Figure 1C), yielding a DNA 3′-phosphate and the native enzyme (Figure 1D). Subsequent processing by polynucleotide kinase phosphatase (PNKP), DNA polymerases, and DNA ligases finishes DNA restoration.[6,7,14] In addition, Tdp1 has also been reported to repair oxidative damage-induced 3′-phosphoglycolates and alkylation damage-induced DNA breaks.[12,15,16] It is believed that by

Received: October 21, 2016

DOI: 10.1021/acs.jmedchem.6b01565
J. Med. Chem. XXXX, XXX, XXX−XXX

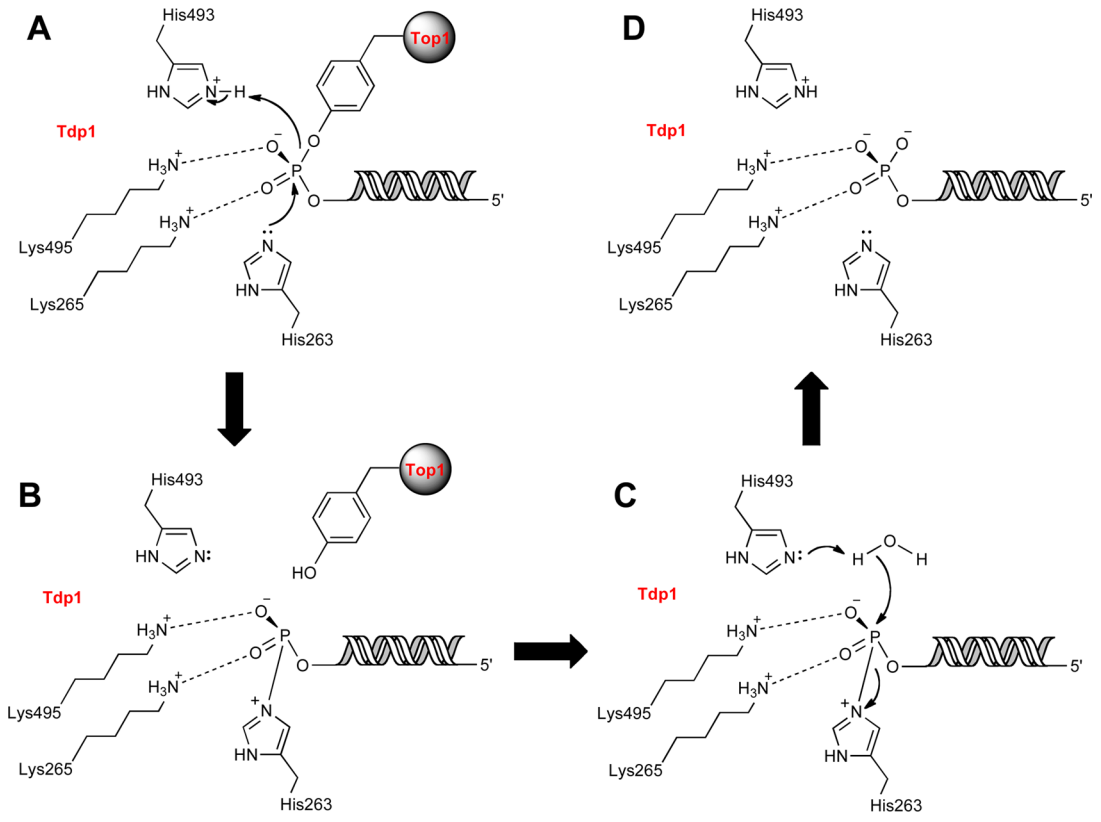

Figure 1. Mechanism proposed for Tdp1.[17] (A) His263 carries out a nucleophilic attack on the DNA-Top1 phosphodiester link, resulting in Tdp1-linked DNA (B). (C) Enzyme-catalyzed hydrolysis of the Tdp1−DNA phosphodiester link involving His493 results in a DNA-3′-phosphate and free enzyme (D).

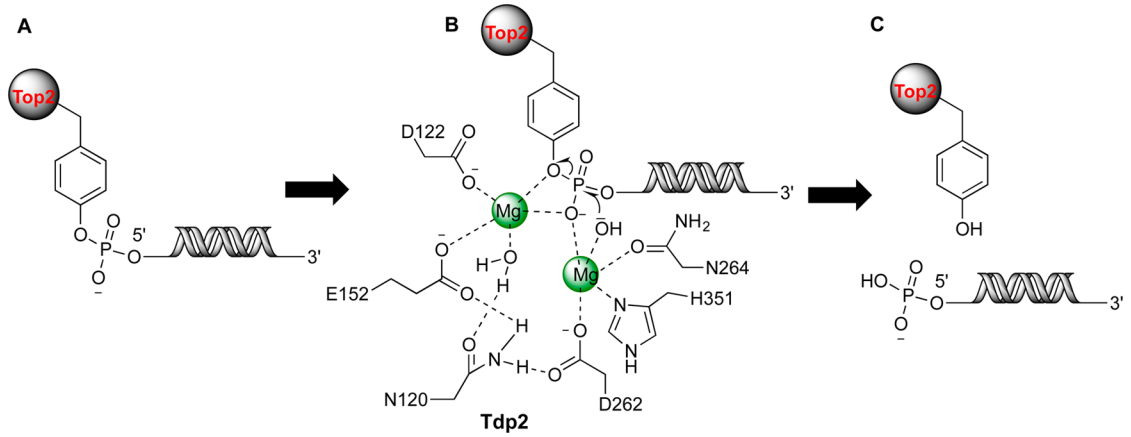

Figure 2. Proposed reaction mechanism for phosphodiester bond cleavage by Tdp2.[23] (A) Top2-derived peptide (trapped topoisomerase) linked to 5′-DNA via a phosphotyrosyl bond. (B) Upon binding of the covalent enzyme−DNA substrate in the Tdp2 active site, two magnesium ions are coordinated by the Tdp2 catalytic residues to activate nucleophilic attack of the phosphotyrosyl bond (curved arrows). (C) Cleavage products consisting of Top2 and the liberated DNA with a 5′-phosphate end.[15]

reducing the repair of Top1−DNA lesions, Tdp1 inhibitors have the potential to augment the anticancer activities of Top1 inhibitors, which makes Tdp1 a rational anticancer drug development target.[15,17,18]

Tyrosyl−DNA phosphodiesterase II (Tdp2) is a member of the metal-dependent phosphodiesterases that was recently discovered with repair function linked to topoisomerase II (Top2)-mediated DNA damage.[15,19,20] Tdp2 cleaves Top2−DNA adducts by catalyzing the hydrolysis of 5′-phosphotyrosyl bonds and thereby releasing trapped Top2 from 5′-termini (Figure 2), thus playing a key role in maintaining normal DNA topology.[15] Inhibition of Tdp2 may therefore be a useful approach to overcome intrinsic or acquired resistance to Top2-targeted drug therapy.[19,20] More recently, it was revealed that Tdp2 also promotes repair of Top1-mediated DNA damage in the absence of Tdp1 and that cells lacking both Tdp1 and Tdp2 are more sensitive to Top1 inhibitors than Tdp1-deficient cells.[21,22] The hypothesis that Tdp2 may serve as a potential therapeutic co-target of Top1 and Tdp1 needs to be tested.[15,19]

The functional relationships among these enzymes make Tdp1 and Tdp2 attractive targets for cancer treatment in combination with Top1 inhibitors, an idea that is also

DOI: 10.1021/acs.jmedchem.6b01565
J. Med. Chem. XXXX, XXX, XXX−XXX

supported by the hypersensitivity of Tdp1- and Tdp2-deficient vertebrate cells to topoisomerase inhibitors.[12,14,19,21,24−29] It has therefore been proposed that combination therapies that target both Tdp1 and Top1 should improve potency and selectivity toward cancer cells with preexisting repair and checkpoint deficiencies.[15] A limited number of Tdp1 and Tdp2 inhibitors have been reported in the literature, but many of them are hampered by problems of chemical or metabolic instability and low potency, or by being PAINS (pan-assay interference) compounds.[8,17,18,28−42] Encouragingly, a series of indenoisoquinoline dual Top1-Tdp1 inhibitors displaying good activity on both Top1 and Tdp1 were recently reported (e.g., compounds **1**−**4** in Figure 3),[43−45] suggesting that chemical modifications of the indenoisoquinoline ring system might allow the generation of dual Top1-Tdp1 inhibitors with optimized potencies.

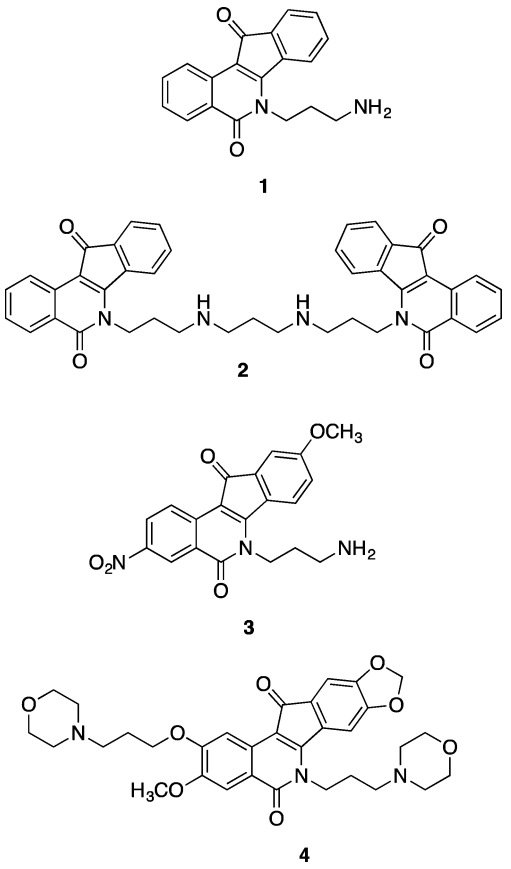

Figure 3. Representative dual Top1-Tdp1 inhibitors.

Compared to indenoisoquinolines, azaindenoisoquinolines offer the possibility of improved drug−Top1−DNA ternary complex stabilization through enhanced charge transfer interactions involving the donation of electron density to the drug from the flanking DNA base pairs.[46−48] Previous studies of azaindenoisoquinolines in which a nitrogen atom was systematically rotated to eight different locations in the two aromatic rings established the 7-position (e.g., in compound **5**) as the one that conferred the greatest potency vs Top1.[46,47] The addition of a methoxy group at the 9 position and a nitro group at the 3 position further improved the potencies of the azaindenoisoquinolines, resulting in compounds with potent Top1 inhibition and cytotoxicity.[48] Encouraged by these reports and others,[21,43,44,49] the present study was initiated to investigate the hypothesis that manipulation of the side chain on the lactam nitrogen in 7-azaindenoisoquinolines could lead to compounds capable of simultaneously inhibiting Top1, Tdp1, and Tdp2. Prior reports on the crystal structures of Top1,[4] Tdp1,[50] and Tdp2[51,52] provided the foundation for a structure-based drug design approach.

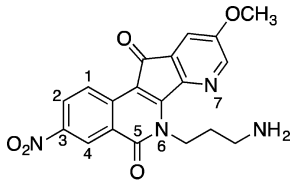

5

RESULTS AND DISCUSSION

Design. Compound **5** was docked in the active sites of the three enzymes Top1 (PDB ID: 1K4T),[4] Tdp1 (PDB ID: 1NOP),[50] and Tdp2 (PDB ID: 5J3S)[52] to investigate the binding modes and the possibilities for modification of the side chain. As expected, the azaindenoisoquinoline scaffold stacked between the base pairs of DNA in the Top1−DNA covalent complex with a hydrogen bond between the ketone carbonyl of the drug and a side chain nitrogen of Arg364 (Figure 4, top). The side chain was directed toward a flexible site in the major groove of DNA that can accommodate a wide range of substituents.

The substrate binding site of Tdp1 is quite large in order to accommodate DNA and a Top1-derived peptide (Figure 4, middle, and Figure 5). The DNA part of the substrate binds to a phenylalanine Phe259 via π stacking while maintaining a network of hydrogen bonds with Arg535, Lys469, and Ser403, and the peptide part of the complex is directed to the catalytic residues deep in the active site (Figure 5). Compound **5** was calculated to adopt a similar binding mode as the substrate in which the 7-azaindenoisoquinoline scaffold stacked with the phenylalanine residue and the side chain occupies the DNA binding pocket pointing toward the catalytic site residues (Figure 4, middle), which are basic and hydrophilic, suggesting the exploration of azaindenoisoquinolines having hydrophilic side chains that incorporate hydrogen bonding groups.

The predicted binding mode of the lead compound **5** in the active site of Tdp2 (Figure 4, bottom) supports the idea to add hydrophilic side chains since the amino group is calculated to be pointed toward a solvent-exposed area. Based on the molecular modeling studies, the present series of 7-azaindenoisoquinolines with various hydrophilic side chains were designed and synthesized to explore the effect of side chain variation on the activity of this class against Top1, Tdp1, and Tdp2.

Chemistry. Preparation of compound **7** was first explored through Mitsunobu reaction by treating **6**[46] with 3-bromopropanol, Ph_3P, and DIAD in THF (Scheme 1), but only a moderate yield (39%) was obtained, and tedious chromatography was required to get pure product. An S_N2 substitution with 1,3-dibromopropane was then investigated to install the 3-bromopropyl side chain. After thorough optimization of the reaction conditions, it was determined that when compound **6** was treated with sodium hydride in anhydrous DMF, followed by addition of sodium iodide (0.1 equiv) and 1,3-dibromopropane at −10 to 0 °C for 30 h, compound **7** could be obtained in 72% yield. This improve-

DOI: 10.1021/acs.jmedchem.6b01565
J. Med. Chem. XXXX, XXX, XXX−XXX

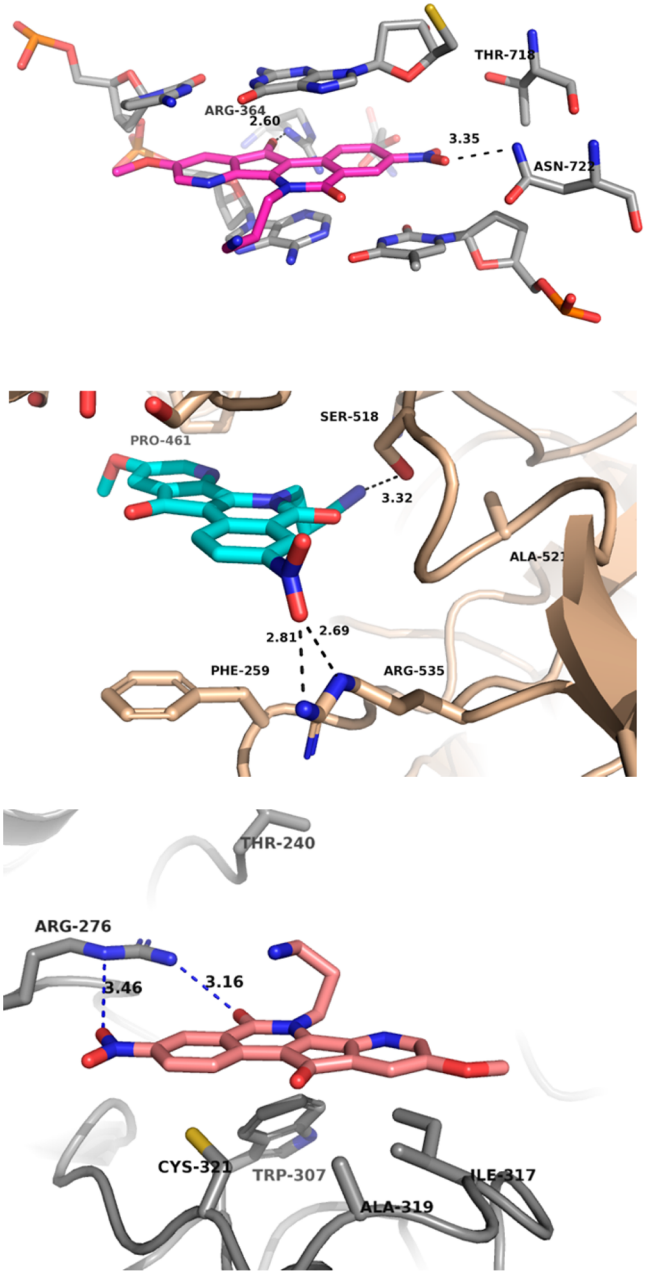

Figure 4. Hypothetical binding modes of 7-azaindenoisoquinoline **5** with Top1[4] (PDB ID: 1K4T) (top), Tdp1[50] (PDB ID: 1NOP) (middle), and Tdp2[52] (PDB ID: 5J3S) (bottom).

ment in yield over the previously reported reaction conditions resulted from the use of NaI.[48] The practical preparation of compound **7** on a gram scale made it possible to synthesize 7-azaindenoisoquinoline analogues with maximum side chain variation, thereby facilitating the structure−activity relationship (SAR) study.

The SAR study was restricted to varying the lactam γ-aminopropyl side chain. As illustrated in Scheme 2, compounds **8**, **9**, **10**, **12**, **13**, **16**, and **17** were prepared in 50−77% yields by heating compound **7** with the corresponding amines at reflux in 1,4-dioxane in the presence of K_2CO_3 and NaI, while compounds **11**, **14**, and **15** were obtained by treatment of **7** with methylamine, isopropylamine, and ethylamine in DMF at room temperature in the presence of triethylamine and 0.1 equiv of NaI in 68%, 80%, and 73% yields, respectively.

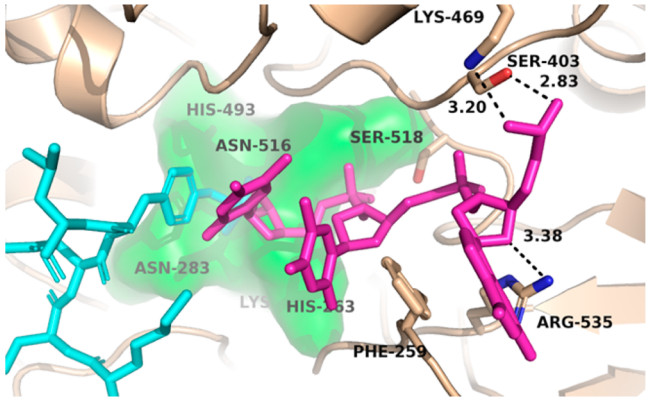

Figure 5. Binding of DNA (magenta) and a Top1-derived, Tyr723-containing octapeptide (cyan) in the active site of Tdp1[50] (PDB ID: 1NOP) (tan). The catalytic residues of the enzyme are displayed in green.

Scheme 1[a]

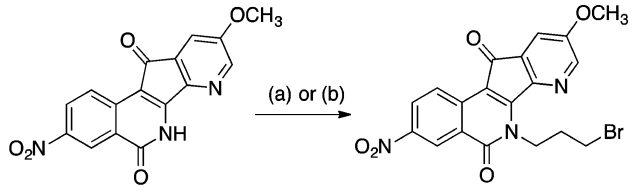

6 **7**

[a]Reagents and conditions: (a) 3-bromopropanol, triphenylphosphine, DIAD, THF, 23 °C, 60 h, 39%; (b) (i) NaH, DMF, 0 to 23 °C, 3 h; (ii) 1,3-dibromopropane, 0.1 equiv NaI, −10 to 0 °C, 30 h, 72%.

Scheme 2[a]

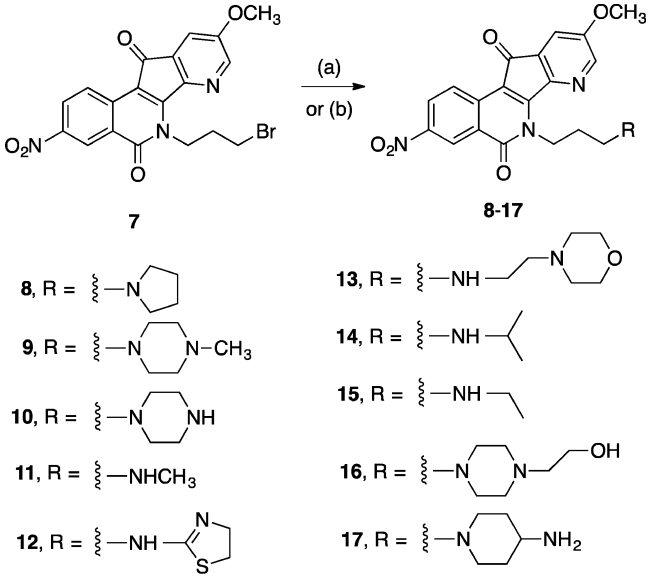

7 **8-17**

[a]Reagents and conditions: (a) amine (pyrrolidine for **8**, 1-methylpiperazine for **9**, piperazine for **10**, 2-amino-2-thiazoline for **12**, and 4-(2-aminoethyl)morpholine for **13**, 1-(2-hydroxyethyl)-piperazine for **16**, and 4-aminopiperidine for **17**), NaI, K_2CO_3, 1,4-dioxane, reflux, 6 h (**8**, 68%; **9**, 77%; **10**, 66%; **12**, 57%; **13**, 50%; **16**, 53%, **17**, 63%); (b) amine (methylamine for **11**, isopropylamine for **14**, ethylamine for **15**), NaI, Et_3N, DMF, room temperature, 12 h (**11**, 68%; **14**, 80%; **15**, 73%).

DOI: 10.1021/acs.jmedchem.6b01565
J. Med. Chem. XXXX, XXX, XXX−XXX

Table 1. Top1, Tdp1, and Tdp2 Inhibitory Activities and Cytotoxicities of 7-Azaindenoisoquinolines

	cytotoxicity (GI_{50}, μM)[a]							enzyme inhibitory activity		
compd	lung HOP-62	CNS SF-539	melanoma UACC-62	ovarian OVCAR-3	renal SN12C	breast MCF-7	MGM	Top1[c]	Tdp1[d]	Tdp2[d]
7	0.058	0.279	0.082	0.248	0.269	0.046	0.112	++	++	+
8	<0.01	0.031	0.015	0.059	0.036	<0.01	0.045	++	+++	+
9	0.081	0.191	0.183	0.171	0.214	0.016	0.562	++	++	++
10	0.065	0.355	0.175	1.190	0.230	0.036	0.316	++	++	+
11	0.030	0.051	0.020	0.174	0.046	1.06	0.741	+++	+++	+
12	0.014	0.036	<0.01	0.137	<0.01	<0.01	0.058	++++	+++	++
13	0.150	0.311	0.044	0.315	0.080	0.032	0.177	+++	++	+
14	0.085	0.051	0.019	0.082	0.039	0.012	0.058	++++	++	+
15	0.107	0.070	0.027	0.062	0.053	0.019	0.079	++++	+++	+
16	2.76	1.70	1.22	1.46		0.142	1.66	+++	0	0
17	NS[b]	NS	NS	NS	NS	NS	NS	++	+++	+++
18	<0.01	<0.01	<0.01	0.22	0.020	0.013	0.040	++++	0	0
19	0.02	0.04	0.03	0.50	<0.01	<0.01	0.21	++++	+/++	+++

[a]The cytotoxicity GI_{50} values listed are the concentrations corresponding to 50% growth inhibition and are the result of single determinations. [b]Not selected for 5-concentration testing due to low cytotoxicity in the one-concentration preliminary testing. [c]Compound-induced DNA cleavage resulting from Top1 inhibition is graded by the following semiquantitative scale relative to 1 μM MJ-III-65 (**19**) and 1 μM camptothecin (**18**): 0, no detectable activity; +, weak activity; ++, activity less than that of MJ-III-65 (**19**); +++, activity equal to that of **19**; ++++, activity equipotent with **18**. [d]Tdp1 and Tdp2 IC_{50} values were determined in duplicate using a semiquantitative scale: 0, IC_{50} > 111 μM; +, IC_{50} between 37 and 111 μM; ++, IC_{50} between 12 and 37 μM; +++, IC_{50} between 1 and 12 μM; ++++, IC_{50} < 1 μM.

Biological Results. All of the synthesized compounds **7**−**17** were tested for their inhibitory activities against Top1, Tdp1, and Tdp2. Their antiproliferative activities were also evaluated against the NCI-60 panel of human cancer cell lines. Top1 inhibition was recorded as the ability of the drug to induce enzyme-linked DNA breaks in the Top1-mediated DNA cleavage assay.[53] The results of this assay are designated relative to the Top1 inhibitory activities of camptothecin (**18**) and MJ-III-65 (**19**, also known as NSC 706744 and LMP744)[54,55] and are expressed in semiquantitative fashion: 0, no detectable activity; +, weak activity; ++, less activity than that of compound **19**; +++, similar activity to that of **19**; ++++, equipotent to **18**. As shown in Table 1 and Figure 6, all of the compounds **7**−**17** exhibited moderate to potent Top1 inhibitory activity. Compound **7** expressed Top1 inhibitory activity at the ++ potency level. Further evaluation of analogues with various amino groups in the side chain (pyrrolidine, **8**; 1-methylpiperazine, **9**; and piperazine, **10**) revealed similar Top1 inhibitory activities at the ++ level. Interestingly, compound **11**, in which a methylamine was introduced at the end of propyl chain, displayed improved Top1 inhibitory activity relative to **7** at the +++ level. Notably, the isopropylamine **14** and ethylamine **15** compounds demonstrated excellent Top1 inhibitory activity at the ++++ level. The 4-(2-aminoethyl)-morpholine compound **13** and 2-amino-2-thiazoline compound **12** displayed improved Top1 inhibitory activity relative to **7** at the +++ and ++++ levels, respectively. The improved potencies of compounds **11**−**15** compared to those of **8**−**10** indicate that a secondary amine in side chain of 7-azaindenoisoquinolines is better than a tertiary amine for the Top1 inhibitory activity.

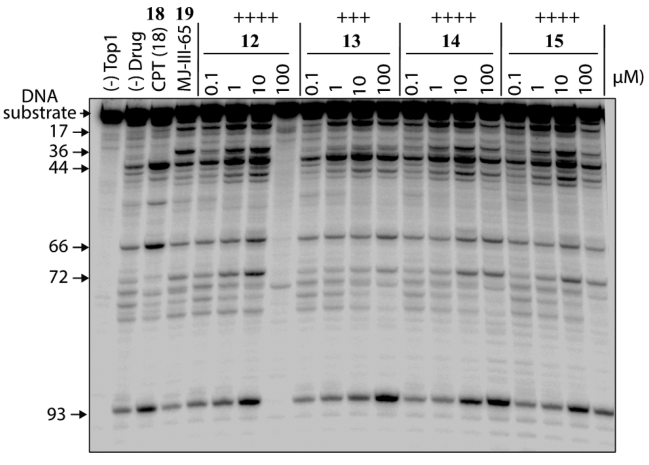

Figure 6. Representative gel showing Top1-mediated DNA cleavage induced by indenoisoquinolines **12**−**15**. From left to right: lane 1, DNA alone; lane 2, DNA + Top1; lane 3, 1 μM camptothecin (CPT, **18**) + DNA + Top 1; lane 4, 1 μM MJ-III-65 (**19**) + DNA + Top1; Lanes 5−20, compounds **12**−**15** (each at 0.1, 1.0, 10, and 100 μM). Numbers and arrows on the left indicate arbitrary cleavage site positions. CPT (**18**) and the indenoisoquinoline MJ-III-65 (**19**) are positive controls.

Top1 inhibitors can be classified as being poisons or suppressors. The Top1 poisons inhibit the DNA religation reaction in the drug−DNA−Top1 ternary complex, while suppressors inhibit the DNA cleavage reaction in which the enzyme forms a covalent bond with the DNA through a phosphodiester linkage. It is apparent from the gel data depicted in Figure 6 that the azaindenoisoquinoline **12** acts as a poison in the 0.1−10 μM range, but it acts as a suppressor at a concentration of 100 μM. This behavior has been routinely observed in both the indenoisoquinoline[43,49] and azaindenoisoquinoline[46,48] series, and most likely results from the binding of the drug to DNA at high drug concentrations, thus making the DNA a poorer substrate. It can be modulated by altering the substituted side chain that is connected to the lactam.

Figure 7 shows the binding mode of compound **12** between the DNA base pairs in the active site of Top1. The 7-azaindenoisoquinoline scaffold is stacked between the base pairs of DNA with a hydrogen bond between the ketone carbonyl and a side chain nitrogen of Arg364. The nitro group hydrogen bonds to the side chain hydroxyl group of Thr718 as well as a side chain N−H of Asn722. The 2-amino-2-thiazoline side chain is directed to a solvent-exposed area in the major groove. The hydrophilic nature of the side chain facilitates the

DOI: 10.1021/acs.jmedchem.6b01565
J. Med. Chem. XXXX, XXX, XXX−XXX

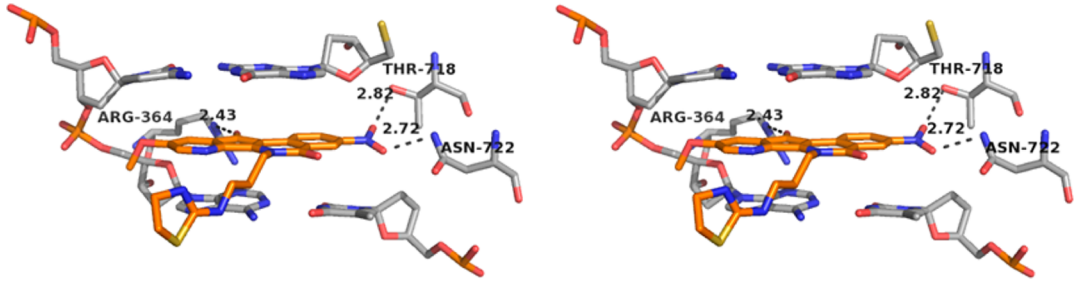

Figure 7. Hypothetical binding mode of compound **12** in ternary complex with DNA and Top1[4] (PDB ID: 1K4T). The stereoview is programmed for walleyed (relaxed) viewing.

binding and stabilization of the 7-azaindenoisoquinoline system between the DNA base pairs.

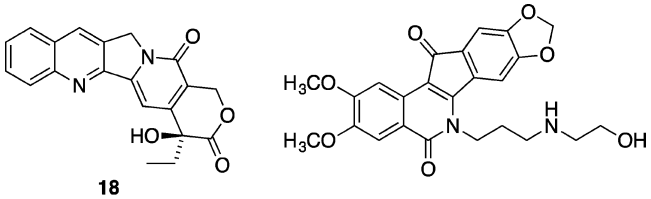

18 **19**

The Tdp1 inhibitory activities of the 7-azaindenoisoquinolines were determined by measuring their abilities to inhibit the hydrolysis of the phosphodiester linkage between the tyrosine residue and the 3′-end of a DNA oligonucleotide substrate (N14Y), thus preventing the generation of an oligonucleotide with a free 3′-phosphate (N14P).[32] Therefore, the disappearance of the gel band for N14P indicates Tdp1 inhibition (Figure 8). The Tdp1 inhibitory activities of the 7-azaindenoisoquinolines are summarized in Table 1, and representative gels demonstrating dose-dependent Tdp1 inhibition are depicted in Figure 8. Tdp1 inhibitory potencies were determined in duplicate using a semiquantitative scale: 0, IC_{50} > 111 μM; +, IC_{50} between 37 and 111 μM; ++, IC_{50} between 12 and 37 μM; +++, IC_{50} between 1 and 12 μM; and ++++, IC_{50} < 1 μM.[44] Compounds **11** and **15**, with methylamine and ethylamine at the end of the side chain, respectively, display good Tdp1 inhibitory activities with +++ potency. Compounds **8** and **12**, with five-membered cyclic amine substituents at the end of their side chains, also exhibit

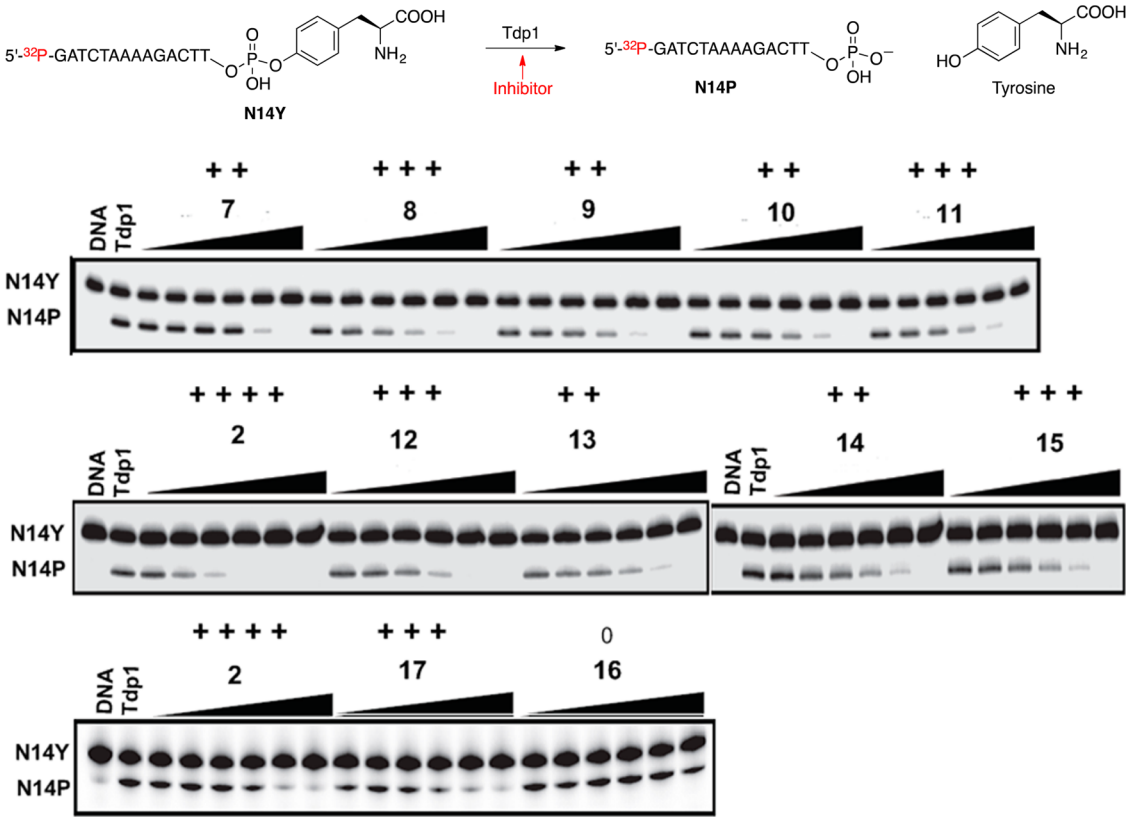

Figure 8. Representative gels showing concentration-dependent Tdp1 inhibition by 7-azaindenoisoquinolines **7**–**17**. From left to right (upper): lane 1, DNA alone; lane 2, DNA + Tdp1; lanes 3–32, DNA + Tdp1 + compounds **7**–**11** (each at 1.4, 4.1, 12.3, 37, and 111 μM). From left to right (middle): lane 1, DNA alone; lane 2, DNA + Tdp1; lanes 3–32, DNA + Tdp1 + compounds AM-8–3 (**2**) and **12**–**15** (each at 1.4, 4.1, 12.3, 37, and 111 μM). From left to right (lower): lane 1, DNA alone; lane 2, DNA + Tdp1; lanes 3–20, DNA + Tdp1 + compounds **2**, **17**, and **16** (each at 1.4, 4.1, 12.3, 37, and 111 μM). Compound **2** is the positive control.

DOI: 10.1021/acs.jmedchem.6b01565
J. Med. Chem. XXXX, XXX, XXX−XXX

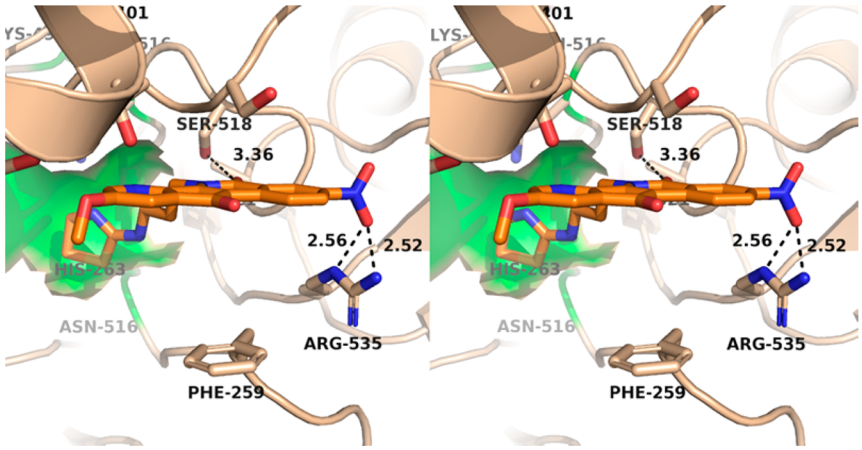

Figure 9. Hypothetical binding mode of compound **12** with Tdp1[50] (PDB ID: 1NOP). The stereoview is programmed for walleyed (relaxed) viewing.

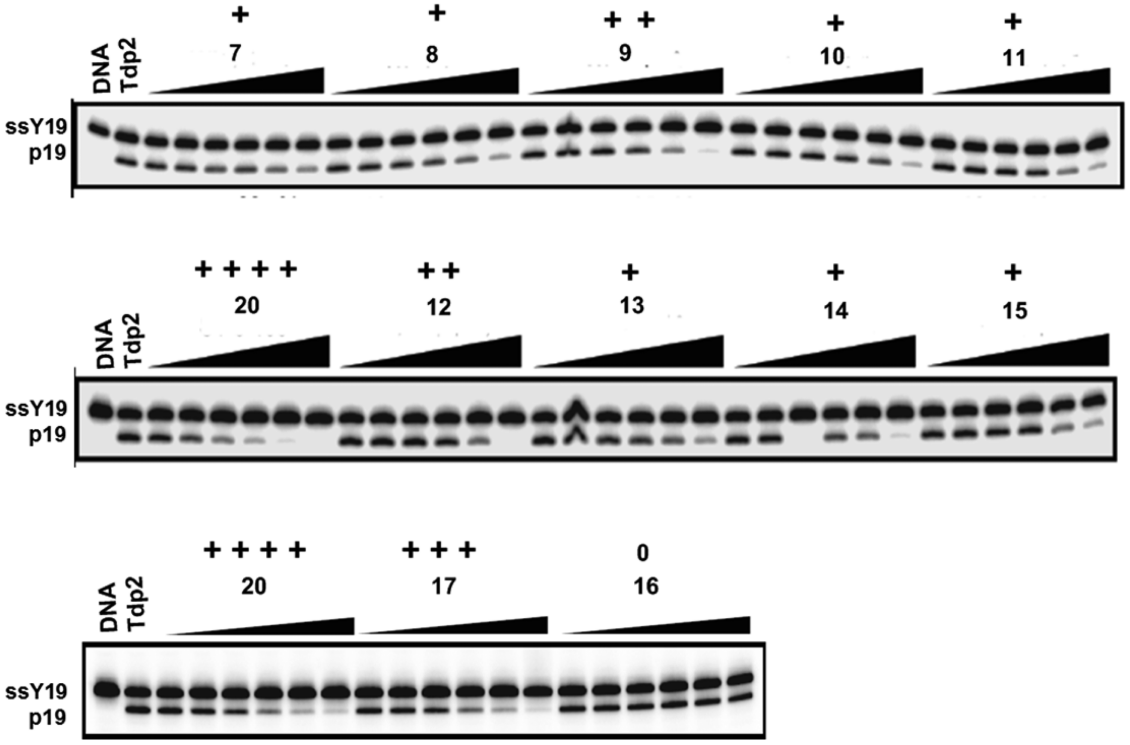

Figure 10. Representative gels showing concentration-dependent Tdp2 inhibition by 7-azaindenoisoquinolines **7**−**17**: From left to right (upper): lane 1, DNA alone; lane 2, DNA + Tdp2; lanes 3−32, DNA + Tdp2 + compounds **7**−**11** (each at 0.46, 1.4, 4.1, 12.3, 37, and 111 μM). From left to right (middle): lane 1, DNA alone; lane 2, DNA + Tdp2; lanes 3−32, DNA + Tdp2 + compound **20** (at 0.017, 0.05, 0.15, 0.46, 1.4, and 4.1 μM) and **12**−**15** (each at 0.46, 1.4, 4.1, 12.3, 37, and 111 μM). From left to right (lower): lane 1, DNA alone; lane 2, DNA + Tdp2; lanes 3−20, DNA + Tdp2 + compound **20** (at 0.017, 0.05, 0.15, 0.46, 1.4, 4.1 μM), **17** and **16** (each at 0.46, 1.4, 4.1, 12.3, 37, and 111 μM). Compound **20** is the positive control.

good inhibition of Tdp1 at the +++ potency level. However, when six-membered cyclic amine or isopropylamine substituents were introduced to the side chain, only moderate Tdp1 inhibitory activities at the ++ level were found for the corresponding compounds **9**, **10**, **13**, and **14**.

Figure 9 illustrates the hypothetical binding mode of compound **12** in the active site of Tdp1. The 7-azaindenoisoquinoline scaffold binds to the Phe259 benzene ring via π stacking, while the nitro group hydrogen bonds with Arg535. The lactam carbonyl oxygen of the scaffold is involved in hydrogen bonding with Ser518, which is an important residue for the binding of the DNA−peptide substrate to the enzyme. Finally, the 2-amino-2-thiazoline side chain of the compound is directed to the deep region of the enzyme (green) where the catalytic residues reside. The hydrophilic nature of this side chain is important for the binding as the catalytic residues are hydrophilic in nature.

The inhibitory effects of these 7-azaindenoisoquinolines on Tdp2 were examined in a similar fashion as Tdp1. As shown in Table 1 and Figure 10, all of the compounds displayed some degree of inhibitory activity vs Tdp2 with potencies varying from the + to the +++ levels. The previously described inhibitor SV-5−153 (**20**, Figure 10) was included as a positive control.[28,38] Compound **17** is the best one with Tdp2

DOI: 10.1021/acs.jmedchem.6b01565
J. Med. Chem. XXXX, XXX, XXX−XXX

inhibitory activity at the +++ level, the highest in this series. Fortunately, the crystal structure of the human Tdp2 (PDB: 5J3S) has just been released and was used for docking studies involving **17**.[52] As demonstrated in Figure 11, the side chain is calculated to be directed toward a solvent exposed area, and the lactam carbonyl oxygen hydrogen bonds to the Arg276 side chain.

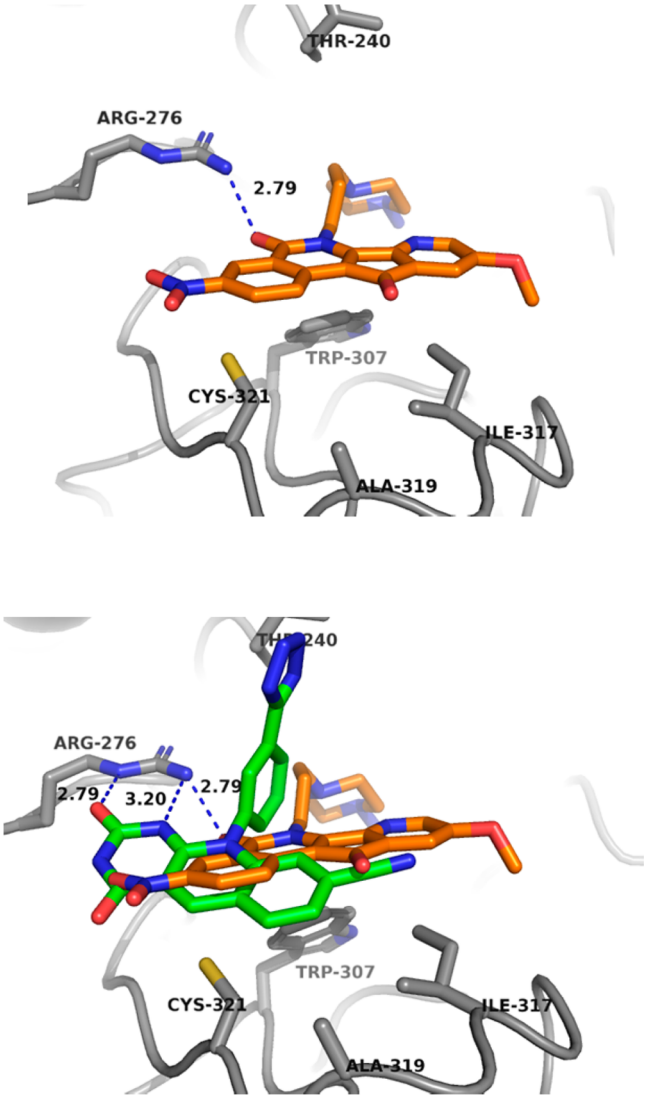

Figure 11. Upper: hypothetical binding mode of compound **17** with Tdp2 (PDB code: 5J3S).[28,38,52] Lower: the structure of **17** (orange) is overlapped with that of **20** (green), which is present in the crystal structure of the enzyme complex with **20**.

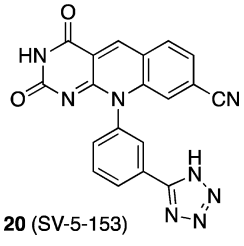

20 (SV-5-153)

To investigate their potential as anticancer agents, the 7-azaindenoisoquinolines **7**−**17** were evaluated in the National Cancer Institute's Developmental Therapeutics Program screen against 60 human cancer cell lines (the "NCI-60").[56] The GI_{50} values obtained with selected cell lines, along with the mean graph midpoint (MGM) values based on all 60 cell lines, are summarized in Table 1. The MGM is based on a calculation of the average GI_{50} values for all of the cell lines tested in which GI_{50} values below and above the test range (0.01 to 100 μM) are taken as the minimum (0.01 μM) and maximum (100 μM) drug concentrations used in the screening test. Many of these new compounds displayed significant potencies against various cell lines with GI_{50} MGMs in the low micromolar to submicromolar range (0.045−1.66 μM). The Top1 ++++ compounds **12**, **14**, and **15** were among the most cytotoxic, with MGM values of 0.058, 0.058, and 0.079 μM, respectively. The differences in cytotoxicity among these three compounds are low despite clear differences in Tdp1 and Tdp2 inhibition, suggesting that Tdp1 and Tdp2 inhibition do not contribute significantly to the cytotoxicities of these compounds. The Top1 +++ compounds are **11** (MGM 0.714 μM), **13** (MGM 0.177 μM), and **16** (MGM 1.650 μM). On the basis of the Tdp1 and Tdp2 inhibitory potencies, **16** is expected to be the least potent, which it clearly is. However, one would expect **11** to be the most cytotoxic, and in fact, **13** is the most cytotoxic of the three compounds. Among the Top1 ++ compounds, **7** (MGM 0.112 μM), **8** (MGM 0.045 μM), **9** (MGM 0.562 μM), **10** (MGM 0.316 μM), and **17** (not tested due to low cytotoxicity in the one-concentration preliminary testing), **17** is expected to be the most cytotoxic on the basis of Tdp1 and Tdp2 inhibition, but it is actually the least cytotoxic. Based on their performance against Top1, Tdp1, and Tdp2, compound **7** or **10** should be the least cytotoxic, but actually **17** is. However, compound **8** is surprisingly the most cytotoxic compound in the whole series despite having relatively moderate Top1 inhibitory activity. Overall, these triple inhibitors are very cytotoxic anticancer agents, but their relative cytotoxicities cannot be rationalized simply on the basis of their inhibitory activities vs the three enzymes. Other factors that could possibly contribute to the lack of agreement between the enzyme inhibitory activities and cytotoxicities of these 7-azaindenoisoquinoline include differences in cellular uptake, distribution within the cell, metabolism, efflux from the cell, off-target effects, and lack of sufficient potency vs Tdp1 and Tdp2 to exert a significant synergistic effect.

In order to contrast the biological activities of the compounds in cancer cells versus normal cells, human lymphoblastic leukemia CCRF-CEM cells were compared to normal lymphocytes (PBMCs) with respect to their sensitivity to DNA damage induced by five 7-azaindenoisoquinolines at two different concentrations. DNA damage was monitored by testing the ability of the drugs to induce the phosphorylation of histone H2AX on serine 139 (γ-H2AX), a well-established marker.[57] As documented in Figure 12, each of the compounds **12**, **14**, **15**, **17**, and **18** (camptothecin) produced a significantly more intense γ-H2AX response in the cancer cells as opposed to normal cells after a 2 h exposure, an effect that was evident at both 1 μM and 100 nM. The results indicate that the new compounds elicit markedly more DNA damage in cancer cells versus normal cells.

CONCLUSIONS

In summary, a series of 7-azaindenoisoquinolines were rationally designed through a structure-based approach and synthesized. Subsequent biological evaluation revealed that all of the compounds except **16** have inhibitory activity vs all three

DOI: 10.1021/acs.jmedchem.6b01565
J. Med. Chem. XXXX, XXX, XXX−XXX

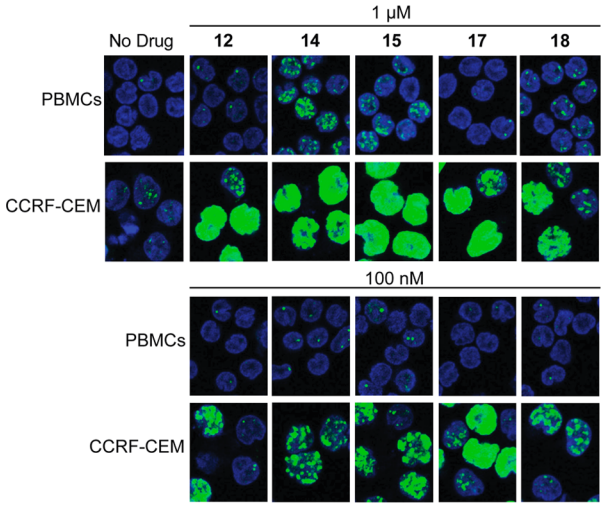

Figure 12. γ-H2AX foci (green) formation in human PBMCs (lymphocytes) and acute lymphoblastic leukemia CCRF-CEM cells treated with indenoisoquinolines **12**, **14**, **15**, **17**, or camptothecin (**18**) at 100 nM (lower panels) and 1 μM (upper panels) for 2 h. Representative confocal microscopy images are shown. DNA was stained with DAPI (blue).

enzymes. Of the tested compounds, the dihydrothiazole derivative **12** displayed the best overall inhibition of Top1, Tdp1, and Tdp2, while the aminopiperidine analogue **17** was found to be the most potent inhibitor of Tdp2. Enzyme inhibitory data and cytotoxicity data from human cancer cell cultures establish that modification of the lactam side chain of the 7-azaindenoisoquinolines can modulate the cytotoxicity and inhibitory potency vs Top1, Tdp1, and Tdp2, and γ-H2AX foci detection experiments indicate greater DNA damage in cancer vs normal cells. The present report proves that it is actually possible to simultaneously inhibit Top1, Tdp1, and Tdp2, and this fact may serve as a springboard to facilitate the elaboration of more potent 7-azaindenoisoquinoline triple inhibitors as potential anticancer agents.

EXPERIMENTAL SECTION

General. NMR spectra were obtained at 300 or 500 (^{1}H) and 75 or 125 (^{13}C) MHz using Bruker ARX300 or Bruker DX-2 500 [QNP probe or multinuclear broadband observe (BBO) probe, respectively] spectrometers. Column chromatography was performed with 230−400 mesh silica gel. The melting points were determined using capillary tubes with a Mel-Temp apparatus and are uncorrected. IR spectra were obtained using a PerkinElmer 1600 series FTIR spectrometer on salt plates or as KBr pellets. ESIMS analyses were recorded on a FinniganMAT LCQ Classic mass spectrometer. APCI−MS analyses were performed using an Agilent 6320 ion trap mass spectrometer. EI/CIMS analyses were obtained with a Hewlett-Packard Engine mass spectrometer. All mass spectral analyses were performed at the Campus-Wide Mass Spectrometry Center of Purdue University. HPLC analyses were carried out on a Waters 1525 binary HPLC pump/Waters 2487 dual λ absorbance detector system using a 5 μm C18 reverse phase column. All reported yields refer to pure isolated compounds. Chemicals and solvents were of reagent grade and used as obtained from commercial sources without further purification. The purities of all of the biologically tested compounds were ≥95% as estimated by HPLC or determined by elemental analysis. For HPLC, the peak area of the major product was ≥95% of the combined total peak areas when monitored by a UV detector at 254 nm.

7-Aza-6-(3-bromopropyl)-5,6-dihydro-9-methoxy-3-nitro-5,11-dioxo-11*H*-indeno[1,2-*c*]isoquinoline (7).[48] Sodium hydride (234 mg, 9.28 mmol) and sodium iodide (70 mg, 0.464 mmol) were added to a suspension of 7-aza-5,6-dihydro-9-methoxy-3-nitro-5,11-dioxo-11*H*-indeno[1,2-*c*]-isoquinoline (**6**, 1.5 g, 4.64 mmol) in dry DMF (230 mL) at 0 °C. After the reaction mixture had been warmed to room temperature and stirred for 3 h, a dark solution formed. The solution was cooled to −10−0 °C in an ice-salt-water bath, and 1,3-dibromopropane (4.686 g, 23.2 mmol) was added. The solution was stirred for 30 h and the reaction quenched with water (200 mL). The product was extracted with ethyl acetate (5 × 200 mL). The combined extracts were washed with water (6 × 150 mL) and brine (3 × 100 mL), dried with sodium sulfate, and evaporated to dryness under reduced pressure. The residue was triturated with ether, filtered, and washed with ether to provide compound **7** as a red solid (1.47 g, 72%): mp 170−172 °C. ^{1}H NMR (300 MHz, $CDCl_3$) δ 9.19 (d, J = 2.4 Hz, 1 H), 8.74 (d, J = 8.9 Hz, 1 H), 8.48 (dd, J = 9.0, 2.3 Hz, 1 H), 8.23 (d, J = 2.6 Hz, 1 H), 7.44 (d, J = 2.7 Hz, 1 H), 5.16−5.05 (m, 2 H), 3.98 (s, 3 H), 3.55 (t, J = 6.8 Hz, 2 H), 2.52−2.37 (m, 2 H); ESIMS m/z (rel intensity) 444.0 (MH^+, 100).

Mitsunobu Approach. 7-Aza-5,6-dihydro-9-methoxy-3-nitro-5,11-dioxo-11*H*-indeno[1,2-*c*]-isoquinoline (**6**, 97 mg, 0.3 mmol) and triphenylphosphine (236 mg, 0.9 mmol) were diluted in THF (30 mL). 3-Bromopropanol (129 mg, 0.9 mmol) was added, followed by DIAD (182 mg, 0.9 mmol). The solution was stirred at room temperature for 60 h, and the reaction mixture was concentrated to dryness. The solid was purified by flash column chromatography, eluting with hexane−ethyl acetate (2:1) to provide the product **7** as a red solid (50 mg, 39%).

7-Aza-5,6-dihydro-6-[3-(4-pyrrolidine-1-yl)propyl]-9-methoxy-3-nitro-5,11-dioxo-11*H*-indeno[1,2-*c*]isoquinoline (8). 7-Aza-6-(3-bromopropyl)-5,6-dihydro-9-methoxy-3-nitro-5,11-dioxo-11*H*-indeno[1,2-*c*]isoquinoline (**7**, 133 mg, 0.3 mmol), pyrrolidine (214 mg, 3 mmol), NaI (10 mg, 0.03 mmol), and potassium carbonate (208 mg, 1.5 mmol) were diluted with 1,4-dioxane (20 mL). The resulting mixture was heated at reflux for 6 h. The solvent was evaporated under reduced pressure, and the residue was redissolved in chloroform (100 mL). The chloroform solution was washed with water (3 × 10 mL) and brine (20 mL), dried with sodium sulfate, and evaporated to dryness. The solid residue was subjected to column chromatography (silica gel), eluting with 5−20% methanol in dichloromethane to yield the red solid product **8** (88 mg, 68%): mp 248−250 °C. IR (film) 3412, 1613, 1483, 1335, 1300 cm^{-1}; ^{1}H NMR (300 MHz, $CDCl_3$) δ 9.17 (d, J = 2.1 Hz, 1 H), 8.78 (d, J = 8.7 Hz, 1 H), 8.52 (dd, J = 9.0, 2.7 Hz, 1 H), 8.27 (d, J = 2.6 Hz, 1 H), 7.45 (d, J = 2.7 Hz, 1 H), 5.07 (t, J = 6.9 Hz, 2 H), 3.99 (s, 3 H), 3.87−3.83 (m, 2 H), 3.28−3.23 (m, 2 H), 2.85−2.80 (m, 2 H), 2.55−2.49 (m, 2 H), 2.28−2.23 (m, 2 H), 2.10−2.0 7 (m, 2 H); ESIMS m/z (rel intensity) 435.1 (MH^+, 100). HPLC purity: 99.42% (C_{18} reverse phase, MeOH-H_2O, 85:15); HRMS-ESI m/z: MH^+ calcd for $C_{23}H_{23}N_4O_5$, 435.1669; found, 435.1656.

Mitsunobu Approach. 7-Aza-5,6-dihydro-9-methoxy-3-nitro-5,11-dioxo-11*H*-indeno[1,2-*c*]-isoquinoline (**6**, 97 mg, 0.3 mmol) and triphenylphosphine (236 mg, 0.9 mmol) were diluted in THF (30 mL). 3-(1-Pyrrolidinyl)-1-propanol (117 mg, 0.9 mmol) was added, followed by DIAD (182 mg, 0.9 mmol). The solution was stirred at room temperature for 72 h. The reaction mixture was concentrated to dryness. The solid was purified by flash column chromatography, eluting with 5−20% methanol in dichloromethane to yield the red solid product **8** (52 mg, 40%).

3-(1-Pyrrolidinyl)-1-propanol. Potassium carbonate (1.4 g, 0.94 mol) and pyrrolidine (0.87 mL, 1.8 mol) were added to a stirred solution of 3-bromopropanol (1 g, 0.635 mol) in 30 mL of THF at 0 °C, and the resulting mixture was stirred at room temperature for 15 h. The resulting mixture was diluted with ethyl acetate (200 mL) and filtered through Celite. The filtrate was concentrated, and the residue was subjected to column chromatography (silica gel), eluting with 50% methanol in dichloromethane, to yield a yellow oil (0.57 g, 70%). ^{1}H NMR (300 MHz, $CDCl_3$) δ 3.79 (t, J = 5.1 Hz, 2 H), 2.71 (t, J = 5.6 Hz, 2 H), 2.57−2.51 (m, 4 H), 1.75−1.66 (m, 6 H); ^{13}C NMR (125 MHz, $CDCl_3$) δ 64.18, 56.02, 54.09, 29.24, 23.27.

7-Aza-5,6-dihydro-6-[3-(3*H*-methylpiperazine-1-yl)propyl]-9-methoxy-3-nitro-5,11-dioxo-11*H*-indeno[1,2-*c*]isoquinoline

DOI: 10.1021/acs.jmedchem.6b01565
J. Med. Chem. XXXX, XXX, XXX−XXX

(9). Compound 7 (133 mg, 0.3 mmol), 1-methylpiperazine (300 mg, 3 mmol), NaI (10 mg, 0.03 mmol), and potassium carbonate (208 mg, 1.5 mmol) were diluted with 1,4-dioxane (20 mL). The resulting mixture was heated at reflux for 6 h. The solvent was evaporated under reduced pressure, and the residue was redissolved in chloroform (100 mL). The chloroform solution was washed with water (3 × 10 mL) and brine (20 mL), dried with sodium sulfate, and evaporated to dryness. The solid residue was subjected to column chromatography (silica gel), eluting with 5−20% methanol in dichloromethane, to yield the orange solid product (107 mg, 77%): mp 211−213 °C. IR (film) 3429, 1666, 1500, 1334, 1286 cm^{-1}; ^1H NMR (300 MHz, $CDCl_3$) δ 9.20 (d, J = 2.3 Hz, 1 H), 8.77 (d, J = 8.9 Hz, 1 H), 8.49 (dd, J = 8.7, 2.6 Hz, 1 H), 8.22 (d, J = 2.6 Hz, 1 H), 7.46 (d, J = 2.7 Hz, 1 H), 5.07 (t, J = 6.9 Hz, 2 H), 3.98 (s, 3 H), 2.60−2.55 (m, 2 H), 2.46−2.28 (m, 8 H), 2.26 (s, 3 H), 2.06−2.01 (m, 2 H); ESIMS m/z (rel intensity) 464.1 (MH^+, 100); HRMS-ESI m/z MH^+ calcd for $C_{24}H_{26}N_5O_5$, 464.1934; found, 464.1928. HPLC purity: 98.34% (C_{18} reverse phase, $MeOH/H_2O$, 90:10).

7-Aza-5,6-dihydro-9-methoxy-3-nitro-5,11-dioxo-6-[3-(piperazine-1-yl)propyl]-11*H*-indeno[1,2-*c*]isoquinoline (10). Compound 7 (133 mg, 0.3 mmol), piperazine (258 mg, 3 mmol), NaI (10 mg, 0.03 mmol), and potassium carbonate (208 mg, 1.5 mmol) were diluted with 1,4-dioxane (20 mL). The resulting mixture was heated at reflux for 6 h. The solvent was evaporated under reduced pressure, and the residue was redissolved in chloroform (100 mL). The chloroform solution was washed with water (3 × 10 mL) and brine (20 mL), dried with sodium sulfate, and evaporated to dryness. The solid residue was subjected to column chromatography (silica gel), eluting with 5−20% methanol in dichloromethane, to yield the red solid product (88 mg, 66%): mp 134−135 °C. IR (film) 3418, 2925, 1671, 1613, 1484, 1336 cm^{-1}; ^1H NMR (300 MHz, $CDCl_3$) δ 9.18 (d, J = 2.4 Hz, 1 H), 8.78 (d, J = 8.8 Hz, 1 H), 8.46 (dd, J = 8.9, 2.6 Hz, 1 H), 8.20 (d, J = 2.5 Hz, 1 H), 7.44 (d, J = 2.8 Hz, 1 H), 5.06 (t, J = 6.8 Hz, 2 H), 3.95 (s, 3 H), 2.58−2.54 (m, 2 H), 2.43−2.25 (m, 8 H), 2.04−1.98 (m, 2 H); 1.91 (brs, 1 H); ESIMS m/z (rel intensity) 450.1 (MH^+, 100); HRMS-ESI m/z MH^+ calcd for $C_{23}H_{23}N_5O_5$, 450.1778; found, 450.1779. HPLC purity: 100% (C_{18} reverse phase, $MeOH/H_2O$, 80:20).

7-Aza-5,6-dihydro-9-methoxy-6-[3-(methylaminopropyl]-3-nitro-5,11-dioxo-11*H*-indeno[1,2-*c*]isoquinoline (11). Compound 7 (133 mg, 0.3 mmol), NaI (10 mg, 0.03 mmol), methylamine (2 M in THF) (3 mL, 6 mmol), and triethylamine (0.125 mL, 0.9 mmol) were diluted with anhydrous DMF (40 mL). The resulting mixture was stirred for 12 h at room temperature and the reaction quenched with water (5 mL). The products were extracted with chloroform (5 × 40 mL). The combined extracts were washed with water (6 × 20 mL) and brine (3 × 20 mL), dried with sodium sulfate, and evaporated to dryness under reduced pressure. The solid residue was subjected to column chromatography (silica gel), eluting with 5−20% methanol in dichloromethane containing 1% trimethylamine, to yield a red solid product (80 mg, 68%): mp 259−262 °C. IR (film) 3435, 2964, 2782, 1682, 1555, 1481, 1336, 1302 cm^{-1}; ^1H NMR (300 MHz, $CDCl_3$) δ 9.18 (d, J = 2.4 Hz, 1 H), 8.75 (d, J = 8.9 Hz, 1 H), 8.48 (dd, J = 8.70, 2.7 Hz, 1 H), 8.23 (d, J = 2.7 Hz, 1 H), 7.43 (d, J = 2.4 Hz, 1 H), 5.03 (t, J = 7.5 Hz, 2 H), 3.97 (s, 3 H), 2.77−2.72 (m, 2 H), 2.45 (s, 3 H), 2.09−1.96 (m, 3 H); ESIMS m/z (rel intensity) 395.1 (MH^+, 100); HRMS-ESI m/z MH^+ calcd for $C_{20}H_{18}N_4O_5$, 395.1356; found, 395.1357. HPLC purity: 96.98% (C_{18} reverse phase, $MeOH/H_2O$, 85:15).

7-Aza-5,6-dihydro-6-[3-((4,5-dihydrothiazol-2-yl)amino)-propyl]-9-methoxy-3-nitro-5,11-dioxo-11*H*-indeno[1,2-*c*]-isoquinoline (12). Compound 7 (106 mg, 0.24 mmol), 2-amino-2-thiazoline (333 mg, 2.4 mmol), NaI (9 mg, 0.024 mmol), and potassium carbonate (165 mg, 1.2 mmol) were diluted with 1,4-dioxane (30 mL). The resulting mixture was heated at reflux for 6 h. The solvent was evaporated under reduced pressure, and the residue was redissolved in chloroform (100 mL). The chloroform solution was washed with water (3 × 10 mL) and brine (20 mL), dried with sodium sulfate, and evaporated to dryness. The solid residue was subjected to column chromatography (silica gel), eluting with 5−20% methanol in dichloromethane, to yield the red solid product (63 mg, 57%): mp 175−177 °C. IR (film) 3430, 1641, 1613, 1504, 1482, 1335 cm^{-1}; ^1H NMR (300 MHz, $CDCl_3$) δ 9.19 (d, J = 2.2 Hz, 1 H), 8.75 (d, J = 8.9 Hz, 1 H), 8.49 (dd, J = 8.9, 2.1 Hz, 1 H), 8.28 (d, J = 2.7 Hz, 1 H), 7.43 (d, J = 2.8 Hz, 1 H), 5.05 (t, J = 5.2 Hz, 2 H), 3.97 (s, 3 H), 3.76 (t, J = 6.7 Hz, 2 H), 3.64 (t, J = 6.5 Hz, 2 H), 3.42 (t, J = 7.5 Hz, 1 H), 3.24 (t, J = 6.7 Hz, 2 H), 2.20−2.15 (m, 2 H); ESIMS m/z (rel intensity) 466.1 (MH^+, 100); HRMS-ESI m/z MH^+ calcd for $C_{22}H_{19}N_5O_5S$, 466.1185; found, 466.1182. HPLC purity: 97.50% (C_{18} reverse phase, $MeOH/H_2O$, 90:10).

7-Aza-5,6-dihydro-9-methoxy-6-[3-((2-morpholinoethyl)-amino)propyl]-3-nitro-5,11-dioxo-11*H*-indeno[1,2-*c*]-isoquinoline (13). Compound 7 (106 mg, 0.24 mmol), 4-(2-aminoethyl)-morpholine (314 mg, 2.4 mmol), NaI (9 mg, 0.024 mmol), and potassium carbonate (165 mg, 1.2 mmol) were diluted with 1,4-dioxane (30 mL). The resulting mixture was heated at reflux for 6 h. The solvent was evaporated under reduced pressure, and the residue was redissolved in chloroform (100 mL). The chloroform solution was washed with water (3 × 10 mL) and brine (20 mL), dried with sodium sulfate, and evaporated to dryness. The solid residue was subjected to column chromatography (silica gel), eluting with 5−20% methanol in dichloromethane, to yield the red solid product (58 mg, 50%): mp 214−216 °C. IR (film) 2770, 1437, 1332, 1219 cm^{-1}; ^1H NMR (300 MHz, $CDCl_3$) δ 9.04 (d, J = 2.2 Hz, 1 H), 8.80 (d, J = 8.9 Hz, 1 H), 8.51 (dd, J = 8.9, 2.1 Hz, 1 H), 8.26 (d, J = 2.7 Hz, 1 H), 7.47 (d, J = 2.8 Hz, 1 H), 4.97 (t, J = 5.3 Hz, 2 H), 3.99 (s, 3 H), 3.94−3.89 (m, 4 H), 3.78 (t, J = 6.5 Hz, 2 H), 3.20−3.15 (m, 2 H), 3.08−3.02 (m, 2 H), 2.80−2.75 (m, 3 H), 2.65 (m, 2 H), 2.22−2.18 (m, 2 H); ESIMS m/z (rel intensity) 494.2 (MH^+, 100); HRMS-ESI m/z MH^+ calcd for $C_{25}H_{27}N_5O_6$, 494.2040; found, 494.2038. HPLC purity: 98.44% (C_{18} reverse phase, $MeOH/H_2O$, 90:10).

7-Aza-5,6-dihydro-6-[3-(isopropylamino)propyl]-9-methoxy-3-nitro-5,11-dioxo-11*H*-indeno[1,2-*c*]isoquinoline (14). Compound 7 (133 mg, 0.3 mmol), NaI (10 mg, 0.03 mmol), isopropylamine (177 mg, 6 mmol), and triethylamine (0.125 mL, 0.9 mmol) were diluted with anhydrous DMF (40 mL). The resulting mixture was stirred for 12 h at room temperature and the reaction quenched with water (5 mL). The products were extracted with chloroform (5 × 40 mL). The combined extracts were washed with water (6 × 20 mL) and brine (3 × 20 mL), dried with sodium sulfate, and evaporated to dryness under reduced pressure. The solid residue was subjected to column chromatography (silica gel), eluting with 5−20% methanol in dichloromethane containing 1% trimethylamine, to yield the red solid product (100 mg, 80%): mp 278−280 °C. IR (film) 2961, 2805, 1677, 1610, 1337, 1288, 854 cm^{-1}; ^1H NMR (300 MHz, DMSO) δ 8.90 (d, J = 2.1 Hz, 1 H), 8.67 (d, J = 8.9 Hz, 1 H), 8.61 (dd, J = 8.8, 2.3 Hz, 1 H), 8.37 (d, J = 2.4 Hz, 1 H), 7.70 (d, J = 2.7 Hz, 1 H), 4.89 (t, J = 7.5 Hz, 2 H), 3.98 (s, 3 H), 3.28−3.21 (m, 1 H), 3.09−3.01 (m, 2 H), 2.16−2.10 (m, 2 H), 1.20 (d, J = 6.5 Hz, 6 H); ESIMS m/z (rel intensity) 423.2 (MH^+, 100); HRMS-ESI m/z MH^+ calcd for $C_{22}H_{22}N_4O_5$, 423.1669; found, 423.1668. HPLC purity: 98.73% (C_{18} reverse phase, $MeOH/H_2O$, 80:20).

7-Aza-6-[3-(ethylamino)propyl]-5,6-dihydro-9-methoxy-3-nitro-5,11-dioxo-11*H*-indeno[1,2-*c*]isoquinoline (15). A mixture of compound 7 (133 mg, 0.3 mmol), anhydrous DMF (35 mL), NaI (10 mg, 0.03 mmol), ethylamine (3 mL of a 2 M solution in THF, 6 mmol), and triethylamine (0.125 mL, 0.9 mmol) was stirred for 12 h at room temperature, and the reaction was then quenched with water (5 mL). The product was extracted with chloroform (6 × 40 mL). The combined extracts were washed with water (5 × 30 mL) and brine (3 × 20 mL), dried with sodium sulfate, and evaporated to dryness under reduced pressure. The solid residue was subjected to column chromatography (silica gel), eluting with 5−20% methanol in dichloromethane containing 1% trimethylamine, to yield the red solid product (89 mg, 73%): mp 266−268 °C. IR (film) 3583, 2946, 1682, 1571, 1482, 1336, 1300 cm^{-1}; ^1H NMR (300 MHz, DMSO) δ 8.89 (d, J = 2.1 Hz, 1 H), 8.65−8.59 (m, 2 H), 8.36 (d, J = 2.6 Hz, 1 H), 7.69 (d, J = 2.7 Hz, 1 H), 4.89 (t, J = 7.5 Hz, 2 H), 3.98 (s, 3 H), 3.08−3.01 (m, 2 H), 2.97−2.89 (m, 2 H), 2.15−2.09 (m, 2 H), 1.17 (t, J = 6.5 Hz, 3 H); MALDI: m/z 409 (MH^+); HRMS-ESI m/z MH^+

DOI: 10.1021/acs.jmedchem.6b01565
J. Med. Chem. XXXX, XXX, XXX−XXX

calcd for $C_{21}H_{20}N_4O_5$, 409.1512; found, 409.1516. HPLC purity: 98.32% (C_{18} reverse phase, MeOH/H_2O, 90:10).

7-Aza-5,6-dihydro-6-[3-(4-(2-hydroxyethyl)piperazin-1-yl)-propyl]-9-methoxy-3-nitro-5,11-dioxo-11*H*-indeno[1,2-*c*]-isoquinoline (16). Compound 7 (133 mg, 0.3 mmol), 1-(2-hydroxyethyl)piperazine (270 mg, 6 mmol), NaI (9 mg, 0.024 mmol), and potassium carbonate (165 mg, 1.2 mmol) were diluted with 1,4-dioxane (30 mL). The resulting mixture was heated at reflux for 6 h. The solvent was evaporated under reduced pressure, and the residue was redissolved in chloroform (120 mL). The chloroform solution was washed with water (3 × 10 mL) and brine (20 mL), dried with sodium sulfate, and evaporated to dryness. The solid residue was subjected to column chromatography (silica gel), eluting with 5−20% methanol in dichloromethane to yield the red solid product (78 mg, 53%): mp 214−216 °C. IR (film) 3439, 1636, 1507, 1483, 1256 cm^{-1}; ^1H NMR (300 MHz, $CDCl_3$) δ 9.20 (d, J = 2.3 Hz, 1 H), 8.76 (d, J = 8.9 Hz, 1 H), 8.50 (dd, J = 8.7, 2.7 Hz, 1 H), 8.21 (d, J = 2.8 Hz, 1 H), 7.44 (d, J = 2.7 Hz, 1 H), 4.90 (t, J = 7.5 Hz, 2 H), 3.98 (s, 3 H), 3.59−3.55 (m, 2 H), 2.97 (t, J = 2.5 Hz, 1 H), 2.59−2.44 (m, 12 H), 2.08−2.03 (m, 2 H); ESIMS m/z (rel intensity) 494.2 (MH^+, 100); HRMS-ESI m/z MH^+ calcd for $C_{25}H_{27}N_5O_6$, 494.2040; found, 494.2041. HPLC purity: 96.97% (C_{18} reverse phase, MeOH/H_2O, 90:10).

6-[3-(4-Aminopiperidin-1-yl)propyl]-7-aza-5,6-dihydro-9-methoxy-3-nitro-5,11-dioxo-11*H*-indeno[1,2-*c*]isoquinoline (17). Compound 7 (133 mg, 0.3 mmol), 4-aminopiperidine (600 mg, 6 mmol), NaI (9 mg, 0.024 mmol), and potassium carbonate (165 mg, 1.2 mmol) were diluted with 1,4-dioxane (30 mL). The resulting mixture was heated at reflux for 6 h. The solvent was evaporated under reduced pressure, and the residue was redissolved in chloroform (140 mL). The chloroform solution was washed with water (3 × 10 mL) and brine (20 mL), dried with sodium sulfate, and evaporated to dryness. The solid residue was subjected to column chromatography (silica gel), eluting with 5−15% methanol in dichloromethane containing 1% trimethylamine to yield the red solid product (87 mg, 63%): mp 258−260 °C. IR (film) 3440, 1641, 1436, 1335, 1301, 1084 cm^{-1}; ^1H NMR (300 MHz, DMSO) δ 8.87 (d, J = 2.2 Hz, 1 H), 8.65−8.57 (m, 3 H), 8.36 (d, J = 2.6 Hz, 1 H), 8.24 (d, J = 2.3 Hz, 1 H), 7.67 (d, J = 2.6 Hz, 1 H), 4.87 (t, J = 7.4 Hz, 2 H), 3.98 (s, 3 H), 2.50−2.39 (m, 7 H), 2.04−1.90 (m, 6 H); ESIMS m/z (rel intensity) 464.1; HRMS-ESI m/z MH^+ calcd for $C_{24}H_{26}N_5O_5$, 464.1934; found, 464.1919. HPLC purity: 95.10% (C_{18} reverse phase, MeOH/H_2O, 80:20).

Molecular Modeling. The PDB files for the X-ray crystal structures of Top1, Tdp1, and Tdp2 were obtained using the protein data bank codes 1K4T, 1NOP, and 5J3S, respectively. The protein structures were cleaned, inspected for errors and missing residues, hydrogens were added, and the water molecules were deleted. The 7-azaindenoisoquinolines were constructed and optimized using ChemDraw and saved in SDF file formats and were corrected using Accelry's Discovery studio 2.5 software. GOLD 4.1 was used for docking with the default parameters except that the iterations were increased to 300 000, and the early termination option was disabled. The centroids of the binding sites were defined by the ligands in the cocrystal structures. The top 10 docking poses per ligand were inspected visually following the docking runs. Energy minimizations were performed for selected ligand poses. The CHARMM force field was utilized within the Accelrys Discovery Studio 2.5 for energy minimization.

Topoisomerase I-Mediated DNA Cleavage Reactions. A 3′-[^{32}P]-labeled 117-bp DNA oligonucleotide was prepared as previously described.[30] The oligonucleotide contains previously identified Top1 cleavage sites in 161-bp pBluescript SK(−) phagemid DNA. Approximately 2 nM radiolabeled DNA substrate was incubated with recombinant Top1 in 20 μL of reaction buffer [10 mM Tris-HCl (pH 7.5), 50 mM KCl, 5 mM $MgCl_2$, 0.1 mM EDTA, and 15 μg/mL BSA] at 25 °C for 20 min in the presence of various concentrations of test compounds. The reactions were terminated by adding SDS (0.5% final concentration) followed by the addition of two volumes of loading dye (80% formamide, 10 mM sodium hydroxide, 1 mM sodium EDTA, 0.1% xylene cyanol, and 0.1% bromophenol blue). Aliquots of each reaction mixture were subjected to 20% denaturing PAGE. Gels were dried and visualized by using a phosphoimager and ImageQuant software (Molecular Dynamics). Cleavage sites are numbered to reflect actual sites on the 117 bp oligonucleotide.[30]

Recombinant Tdp1 Assay.[33,45] A 5′-[^{32}P]-labeled single-stranded DNA oligonucleotide containing a 3′-phosphotyrosine (N14Y) was incubated at 1 nM with 10 pM recombinant Tdp1 in the absence or presence of inhibitor for 15 min at room temperature in the LMP1 assay buffer containing 50 mM Tris HCl, pH 7.5, 80 mM KCl, 2 mM EDTA, 1 mM DTT, 40 μg/mL BSA, and 0.01% Tween-20. Reactions were terminated by the addition of 1 volume of gel loading buffer [99.5% (v/v) formamide, 5 mM EDTA, 0.01% (w/v) xylene cyanol, and 0.01% (w/v) bromophenol blue]. Samples were subjected to a 16% denaturing PAGE with multiple loadings at 12 min intervals. Gels were dried and exposed to a PhosphorImager screen (GE Healthcare). Gel images were scanned using a Typhoon 8600 (GE Healthcare), and densitometry analyses were performed using the ImageQuant software (GE Healthcare).

Recombinant Tdp2 Assay.[23] Tdp2 reactions were carried out as described previously with the following modifications. The 18-mer single-stranded oligonucleotide DNA substrate (TY18, $\alpha^{32}P$-cordycepin-3′-labeled) was incubated at 1 nM with 25 pM recombinant human Tdp2 in the absence or presence of inhibitor for 15 min at room temperature in the LMP2 assay buffer containing 50 mM Tris-HCl, pH 7.5, 80 mM KCl, 5 mM $MgCl_2$, 0.1 mM EDTA, 1 mM DTT, 40 μg/mL BSA, and 0.01% Tween 20. Reactions were terminated and treated similarly to recombinant Tdp1 reactions (see above).

γ-H2AX Detection. Purified lymphocytes were obtained from the NIH blood bank from paid healthy volunteers who gave written informed consent to participate in an IRB-approved study for the collection of blood samples for in vitro research use. The protocol is designed to protect subjects from research risks as defined in 45CFR46 and to abide by all internal NIH guidelines for human subjects research (protocol number 99-CC-0168). The lymphocytes were separated from residual red blood cells using Ficoll gradient (GE Healthcare, Pittsburgh, PA, USA) following the manufacturer's instructions. Cells were maintained in RPMI medium (Thermo Fischer Scientific, Waltham, MA USA) supplemented with 10% fetal bovine serum (Thermo Fischer Scientific, Waltham, MA USA) and 100 U/mL penicillin, 100 mg/mL streptomycin (Thermo Fischer Scientific, Waltham, MA USA) at 37 °C and 5% CO_2.

γ-H2AX staining was performed as described.[58] Briefly, lymphocytes (peripheral mononuclear blood cells/PMBCs) or human acute lymphoblastic leukemia CCRF-CEM cells (2 mil/mL in RPMI 1640 medium supplemented with 10% fetal bovine serum and 100 units/mL penicillin and 100 μg/mL streptomycin) were treated with drugs at 100 nM and 1 μM concentrations for 2 h at 37 °C. After incubation cells were fixed in 2% paraformaldehyde in phosphate-buffered saline (PBS) for 20 min at 23 °C, washed three times with PBS, and resuspended in PBS at 2 mil/mL. Cells (200 μL aliquots at 2 mil/mL) were attached to the slide using Cytospin (800 rpm/4 min) and blocked with 5% bovine serum albumin in PBS-TT (PBS containing 0.5% Tween 20 and 0.1% Triton X-100). Blocked cells were treated with γ-H2AX antibody (abcam cat.# 05-636; dilution 1:500) in 1% BSA (bovine serum albumin) in PBS-TT for 2 h in humid chamber, followed by three 5 min washes with PBS. Cells were then incubated with secondary antibody (goat anti mouse conjugated to Alexa Fluor 488 dye: dilution 1:500, Life Technologies A11029) in 1% BSA in PBS-TT, followed by followed by two 5 min washes with PBS. Slides were mounted with mounting medium containing DAPI and viewed with confocal microscope. The projections were saved as TIFF files.

■ ASSOCIATED CONTENT

Supporting Information

The Supporting Information is available free of charge on the ACS Publications website at DOI: 10.1021/acs.jmedchem.6b01565.

SMILES molecular formula strings (CSV)

DOI: 10.1021/acs.jmedchem.6b01565
J. Med. Chem. XXXX, XXX, XXX−XXX

PDB files of **5** with 1K4T (PDB), 1NOP (PDB), and 5J3S (PDB)
PDB file of DNA and a Top1-derived, Tyr723-containing octapeptide with 1NOP (PDB)
PDB file of **12** in ternary complex with DNA and 1K4T (PDB)
PDB file of **12** with 1NOP (PDB)
PDB file of **17** with 5J3S (PDB)
PDB file of **17** and **20** with 5J3S (PDB)

AUTHOR INFORMATION

Corresponding Author

*Phone: 765-494-1465. Fax: 765-494-6970. E-mail: cushman@purdue.edu.

ORCID

Mark Cushman: 0000-0002-0152-5891

Notes

The authors declare no competing financial interest.

ACKNOWLEDGMENTS

This work was made possible by the National Institutes of Health (NIH) through support with Research Grants U01CA089566 and P30CACA023168. This research was also supported in part by the Intramural Research Program of the NIH, National Cancer Institute, Center for Cancer Research. In vitro cytotoxicity testing was performed by the Developmental Therapeutics Program at the National Cancer Institute, under contract NO1-CO-56000.

ABBREVIATIONS USED

CPT, camptothecin; Top1, topoisomerase IB; Tdp1, tyrosyl−DNA phosphodiesterase 1; Tdp2, tyrosyl−DNA phosphodiesterase 2

REFERENCES

(1) Staker, B. L.; Feese, M. D.; Cushman, M.; Pommier, Y.; Zembower, D.; Stewart, L.; Burgin, A. B. Structures of Three Classes of Anticancer Agents Bound to the Human Topoisomerase I-DNA Covalent Complex. *J. Med. Chem.* **2005**, *48*, 2336−2345.

(2) Pommier, Y.; Cushman, M. The Indenoisoquinoline Noncamptothecin Topoisomerase I Inhibitors: Update and Perspectives. *Mol. Cancer Ther.* **2009**, *8*, 1008−1014.

(3) Ioanoviciu, A.; Antony, S.; Pommier, Y.; Staker, B. L.; Stewart, L.; Cushman, M. Synthesis and Mechanism of Action Studies of a Series of Norindenoisoquinoline Topoisomerase I Poisons Reveal an Inhibitor with a Flipped Orientation in the Ternary DNA-Enzyme-Inhibitor Complex as Determined by X-ray Crystallographic Analysis. *J. Med. Chem.* **2005**, *48*, 4803−4814.

(4) Staker, B. L.; Hjerrild, K.; Feese, M. D.; Behnke, C. A.; Burgin, A. B.; Stewart, L. The Mechanism of Topoisomerase I Poisoning by a Camptothecin Analog. *Proc. Natl. Acad. Sci. U. S. A.* **2002**, *99*, 15387−15392.

(5) Pommier, Y.; Marchand, C. Interfacial Inhibitors: Targeting Macromolecular Complexes. *Nat. Rev. Drug Discovery* **2012**, *11*, 25−36.

(6) Pommier, Y.; Barcelo, J. A.; Rao, V. A.; Sordet, O.; Jobson, A. G.; Thibaut, L.; Miao, Z. H.; Seiler, J. A.; Zhang, H.; Marchand, C.; Agama, K.; Nitiss, J. L.; Redon, C. *Repair of Topoisomerase I-Mediated DNA Damage*; Elsevier: Amsterdam, 2006; Vol. *81*, pp 179−229.

(7) Plo, I.; Liao, Z. Y.; Barcelo, J. M.; Kohlhagen, G.; Caldecott, K. W.; Weinfeld, M.; Pommier, Y. Association of XRCC1 and Tyrosyl DNA Phosphodiesterase (Tdp1) for the Repair of Topoisomerase I-Mediated DNA Lesions. *DNA Repair* **2003**, *2*, 1087−1100.

(8) Davies, D. R.; Interthal, H.; Champoux, J. J.; Hol, W. G. J. Insights into Substrate Binding and Catalytic Mechanism of Human Tyrosyl-DNA Phosphodiesterase (Tdp1) from Vanadate and Tungstate-inhibited Structures. *J. Mol. Biol.* **2002**, *324*, 917−932.

(9) Perego, P.; Cossa, G.; Tinelli, S.; Corna, E.; Carenini, N.; Gatti, L.; De Cesare, M.; Ciusani, E.; Zunino, F.; Luison, E.; Canevari, S.; Zaffaroni, N.; Beretta, G. L. Role of Tyrosyl-DNA Phosphodiesterase 1 and Inter-players in Regulation of Tumor Cell Sensitivity to Topoisomerase I Inhibition. *Biochem. Pharmacol.* **2012**, *83*, 27−36.

(10) Interthal, H.; Pouliott, J. J.; Champoux, J. J. The Tyrosyl-DNA Phosphodiesterase Tdp1 Is a Member of the Phospholipase D Superfamily. *Proc. Natl. Acad. Sci. U. S. A.* **2001**, *98*, 12009−12014.

(11) Raymond, A. C.; Rideout, M. C.; Staker, B.; Hjerrild, K.; Burgin, A. B. Analysis of Human Tyrosyl-DNA Phosphodiesterase I Catalytic Residues. *J. Mol. Biol.* **2004**, *338*, 895−906.

(12) Murai, J.; Huang, S. Y. N.; Das, B. B.; Dexheimer, T. S.; Takeda, S.; Pommier, Y. Tyrosyl-DNA Phosphodiesterase 1 (TDP1) Repairs DNA Damage Induced by Topoisomerases I and II and Base Alkylation in Vertebrate Cells. *J. Biol. Chem.* **2012**, *287*, 12848−12857.

(13) Huang, S. Y. N.; Murai, J.; Dalla Rosa, I.; Dexheimer, T. S.; Naumova, A.; Gmeiner, W. H.; Pommier, Y. TDP1 Repairs Nuclear and Mitochondrial DNA Damage Induced by Chain-terminating Anticancer and Antiviral Nucleoside Analogs. *Nucleic Acids Res.* **2013**, *41*, 7793−7803.

(14) El-Khamisy, S. F.; Saifi, G. M.; Weinfeld, M.; Johansson, F.; Helleday, T.; Lupski, J. R.; Caldecott, K. W. Defective DNA Single-strand Break Repair in Spinocerebellar Ataxia with Axonal Neuropathy-1. *Nature* **2005**, *434*, 108−113.

(15) Pommier, Y.; Huang, S. N.; Gao, R.; Das, B. B.; Murai, J.; Marchand, C. Tyrosyl-DNA-phosphodiesterases (TDP1 and TDP2). *DNA Repair* **2014**, *19*, 114−129.

(16) Inamdar, K. V.; Pouliot, J. J.; Zhou, T.; Lees-Miller, S. P.; Rasouli-Nia, A.; Povirk, L. F. Conversion of Phosphoglycolate to Phosphate termini on 3′ Overhangs of DNA Double Strand Breaks by the Human Tyrosyl-DNA Phosphodiesterase hTdp1. *J. Biol. Chem.* **2002**, *277*, 27162−27168.

(17) Dexheimer, T. S.; Antony, S.; Marchand, C.; Pommier, Y. Tyrosyl-DNA Phosphodiesterase As a Target for Anticancer Therapy. *Anti-Cancer Agents Med. Chem.* **2008**, *8*, 381−389.

(18) Huang, S. Y. N.; Pommier, Y.; Marchand, C. Tyrosyl-DNA Phosphodiesterase 1 (Tdp1) Inhibitors. *Expert Opin. Ther. Pat.* **2011**, *21*, 1285−1292.

(19) Zeng, Z. H.; Cortes-Ledesma, F.; El Khamisy, S. F.; Caldecott, K. W. TDP2/TTRAP Is the Major 5′-Tyrosyl DNA Phosphodiesterase Activity in Vertebrate Cells and Is Critical for Cellular Resistance to Topoisomerase II-induced DNA Damage. *J. Biol. Chem.* **2011**, *286*, 403−409.

(20) Ledesma, F. C.; El Khamisy, S. F.; Zuma, M. C.; Osborn, K.; Caldecott, K. W. A Human 5′-Tyrosyl DNA Phosphodiesterase that Repairs Topoisomerase-Mediated DNA Damage. *Nature* **2009**, *461*, 674−678.

(21) Zeng, Z.; Sharma, A.; Ju, L.; Murai, J.; Umans, L.; Vermeire, L.; Pommier, Y.; Takeda, S.; Huylebroeck, D.; Caldecott, K. W.; El-Khamisy, S. F. TDP2 Promotes Repair of Topoisomerase I-Mediated DNA Damage in the Absence of TDP1. *Nucleic Acids Res.* **2012**, *40*, 8371−8380.

(22) Maede, Y.; Shimizu, H.; Fukushima, T.; Kogame, T.; Nakamura, T.; Miki, T.; Takeda, S.; Pommier, Y.; Murai, J. Differential and Common DNA Repair Pathways for Topoisomerase I- and II-Targeted Drugs in a Genetic DT40 Repair Cell Screen Panel. *Mol. Cancer Ther.* **2014**, *13*, 214−220.

(23) Gao, R.; Huang, S.-y. N.; Marchand, C.; Pommier, Y. Biochemical Characterization of Human Tyrosyl-DNA Phosphodiesterase 2 (TDP2/TTRAP) A Mg^{2+}/Mn^{2+}-dependent Phosphodiesterase Specific for the Repair of Topoisomerase Cleavage Complexes. *J. Biol. Chem.* **2012**, *287*, 30842−30852.

(24) Miao, Z. H.; Agama, K.; Sordet, O.; Povirk, L.; Kohn, K. W.; Pommier, Y. Hereditary Ataxia SCAN1 Cells Are Defective for the

DOI: 10.1021/acs.jmedchem.6b01565
J. Med. Chem. XXXX, XXX, XXX−XXX

Repair of Transcription-dependent Topoisomerase I Cleavage Complexes. *DNA Repair* **2006**, *5*, 1489−1494.
(25) Katyal, S.; El-Khamisy, S. F.; Russell, H. R.; Li, Y.; Ju, L.; Caldecott, K. W.; McKinnon, P. J. TDP1 Facilitates Chromosomal Single-strand Break Repair in Neurons and Is Neuroprotective In Vivo. *EMBO J.* **2007**, *26*, 4720−4731.
(26) Gomez-Herreros, F.; Schuurs-Hoeijmakers, J. H. M.; McCormack, M.; Greally, M. T.; Rultenl, S.; Romero-Granados, R.; Counihan, T. J.; Chaila, E.; Conroy, J.; Ennis, S.; Delanty, N.; Cortes-Ledesma, F.; de Brouwer, A. P. M.; Cavallerit, G. L.; El-Khamisy, S. F.; de Vries, B. B. A.; Caldecott, K. W. TDP2 Protects Tanscription from Abortive Topoisomerase Activity and Is Required for Normal Neural Function. *Nat. Genet.* **2014**, *46*, 516−521.
(27) Gomez-Herreros, F.; Romero-Granados, R.; Zeng, Z. H.; Alvarez-Quilon, A.; Quintero, C.; Ju, L. M.; Umans, L.; Vermeire, L.; Huylebroeck, D.; Caldecott, K. W.; Cortes-Ledesma, F. TDP2-Dependent Non-Homologous End-Joining Protects against Topoisomerase II-Induced DNA Breaks and Genome Instability in Cells and In Vivo. *PLoS Genet.* **2013**, *9* (3), e1003226.
(28) Marchand, C.; Abdelmalak, M.; Kankanala, J.; Huang, S. Y.; Kiselev, E.; Fesen, K.; Kurahashi, K.; Sasanuma, H.; Takeda, S.; Aihara, H.; Wang, Z. Q.; Pommier, Y. Deazaflavin Inhibitors of Tyrosyl-DNA Phosphodiesterase 2 (TDP2) Specific for the Human Enzyme and Active against Cellular TDP2. *ACS Chem. Biol.* **2016**, *11*, 1925−1933.
(29) Kont, Y. S.; Dutta, A.; Mallisetty, A.; Mathew, J.; Minas, T.; Kraus, C.; Dhopeshwarkar, P.; Kallakury, B.; Mitra, S.; Uren, A.; Adhikari, S. Depletion of Tyrosyl DNA Phosphodiesterase 2 Activity Enhances Etoposide-Mediated Double-Strand Break Formation and Cell Killing. *DNA Repair* **2016**, *43*, 38−47.
(30) Antony, S.; Marchand, C.; Stephen, A. G.; Thibaut, L.; Agama, K. K.; Fisher, R. J.; Pommier, Y. Novel High-Throughput Electrochemiluminescent Assay for Identification of Human Tyrosyl-DNA Phosphodiesterase (Tdp1) Inhibitors and Characterization of Furamidine (NSC 305831) as an Inhibitor of Tdp1. *Nucleic Acids Res.* **2007**, *35*, 4474−4484.
(31) Liao, Z. Y.; Thibaut, L.; Jobson, A.; Pommier, Y. Inhibition of Human Tyrosyl-DNA Phosphodiesterase by Aminoglycoside Antibiotics and Ribosome Inhibitors. *Mol. Pharmacol.* **2006**, *70*, 366−372.
(32) Dexheimer, T. S.; Gediya, L. K.; Stephen, A. G.; Weidlich, I.; Antony, S.; Marchand, C.; Interthal, H.; Nicklaus, M.; Fisher, R. J.; Njar, V. C.; Pommier, Y. 4-Pregnen-21-ol-3,20-dione-21-(4-bromobenzenesulfonate) (NSC 88915) and Related Novel Steroid Derivatives as Tyrosyl-DNA Phosphodiesterase (Tdp1) Inhibitors. *J. Med. Chem.* **2009**, *52*, 7122−7131.
(33) Marchand, C.; Lea, W. A.; Jadhav, A.; Dexheimer, T. S.; Austin, C. P.; Inglese, J.; Pommier, Y.; Simeonov, A. Identification of Phosphotyrosine Mimetic Inhibitors of Human Tyrosyl-DNA Phosphodiesterase I by a Novel AlphaScreen High-throughput Assay. *Mol. Cancer Ther.* **2009**, *8*, 240−248.
(34) Takagi, M.; Ueda, J.-y.; Hwang, J.-H.; Hashimoto, J.; Izumikawa, M.; Murakami, H.; Sekido, Y.; Shin-ya, K. Tyrosyl-DNA Phosphodiesterase 1 Inhibitor from an Anamorphic Fungus. *J. Nat. Prod.* **2012**, *75*, 764−767.
(35) Weidlich, I. E.; Dexheimer, T.; Marchand, C.; Antony, S.; Pommier, Y.; Nicklaus, M. C. Virtual Screening using Ligand-based Pharmacophores for Inhibitors of Human Tyrosyl-DNA Phosphodiesterase (hTdp1). *Bioorg. Med. Chem.* **2010**, *18*, 2347−2355.
(36) Sirivolu, V. R.; Vernekar, S. K. V.; Marchand, C.; Naumova, A.; Chergui, A.; Renaud, A.; Stephen, A. G.; Chen, F.; Sham, Y. Y.; Pommier, Y.; Wang, Z. 5-Arylidenethioxothiazolidinones as Inhibitors of Tyrosyl−DNA Phosphodiesterase I. *J. Med. Chem.* **2012**, *55*, 8671−8684.
(37) Weidlich, I. E.; Dexheimer, T.; Marchand, M. A.; Antony, S.; Pommier, Y.; Nicklaus, M. C. Virtual Screening Using Ligand-based Pharmacophores for Inhibitors of Human Tyrosyl-DNA Phospodiesterase (hTdp1). *Bioorg. Med. Chem.* **2010**, *18*, 2347−2355.
(38) Raoof, A.; Depledge, P.; Hamilton, N. M.; Hamilton, N. S.; Hitchin, J. R.; Hopkins, G. V.; Jordan, A. M.; Maguire, L. A.; McGonagle, A. E.; Mould, D. P.; Rushbrooke, M.; Small, H. F.; Smith, K. M.; Thomson, G. J.; Turlais, F.; Waddell, I. D.; Waszkowycz, B.; Watson, A. J.; Ogilvie, D. J. Toxoflavins and Deazaflavins as the First Reported Selective Small Molecule Inhibitors of Tyrosyl-DNA Phosphodiesterase II. *J. Med. Chem.* **2013**, *56*, 6352−6370.
(39) Zakharenko, A. L.; Ponomarev, K. U.; Suslov, E. V.; Korchagina, D. V.; Volcho, K. P.; Vasil'eva, I. A.; Salakhutdinov, N. F.; Lavrik, O. I. Inhibitory Properties of Nitrogen-Containing Adamantane Derivatives with Monoterpenoid Fragments against Tyrosyl-DNA Phosphodiesterase 1. *Russ. J. Bioorg. Chem.* **2015**, *41*, 657−662.
(40) Zakharenko, A.; Khomenko, T.; Zhukova, S.; Koval, O.; Zakharova, O.; Anarbaev, R.; Lebedeva, N.; Korchagina, D.; Komarova, N.; Vasiliev, V.; Reynisson, J.; Volcho, K.; Salakhutdinov, N.; Lavrik, O. Synthesis and Biological Evaluation of Novel Tyrosyl-DNA Phosphodiesterase 1 Inhibitors with a Benzopentathiepine Moiety. *Bioorg. Med. Chem.* **2015**, *23*, 2044−2052.
(41) Arabshahi, H. J.; van Rensburg, M.; Pilkington, L. I.; Jeon, C. Y.; Song, M.; Gridel, L. M.; Leung, E.; Barker, D.; Vuica-Ross, M.; Volcho, K. P.; Zakharenko, A. L.; Lavrik, O. I.; Reynisson, J. A Synthesis, In Silico, In Vitro and In Vivo Study of Thieno[2,3-*b*]pyridine Anticancer Analogues. *MedChemComm* **2015**, *6*, 1987−1997.
(42) Khomenko, T.; Zakharenko, A.; Odarchenko, T.; Arabshahi, H. J.; Sannikova, V.; Zakharova, O.; Korchagina, D.; Reynisson, J.; Volcho, K.; Salakhutdinov, N.; Lavrik, O. New Inhibitors of Tyrosyl-DNA Phosphodiesterase I (Tdp 1) Combining 7-Hydroxycoumarin and Monoterpenoid Moieties. *Bioorg. Med. Chem.* **2016**, *24*, 5573−5581.
(43) Lv, P. C.; Agama, K.; Marchand, C.; Pommier, Y.; Cushman, M. Design, Synthesis, and Biological Evaluation of O-2-Modified Indenoisoquinolines as Dual Topoisomerase I-Tyrosyl-DNA Phosphodiesterase I Inhibitors. *J. Med. Chem.* **2014**, *57*, 4324−4336.
(44) Conda-Sheridan, M.; Reddy, P. V. N.; Morrell, A.; Cobb, B. T.; Marchand, C.; Agama, K.; Chergui, A.; Renaud, A.; Stephen, A. G.; Bindu, L. K.; Pommier, Y.; Cushman, M. Synthesis and Biological Evaluation of Indenoisoquinolines That Inhibit Both Tyrosyl-DNA Phosphodiesterase I (Tdp1) and Topoisomerase I (Top1). *J. Med. Chem.* **2013**, *56*, 182−200.
(45) Nguyen, T. X.; Morrell, A.; Conda-Sheridan, M.; Marchand, C.; Agama, K.; Bermingam, A.; Stephen, A. G.; Chergui, A.; Naumova, A.; Fisher, R.; O'Keefe, B. R.; Pommier, Y.; Cushman, M. Synthesis and Biological Evaluation of the First Dual Tyrosyl-DNA Phosphodiesterase I (Tdp1)-Topoisomerase I (Top1) Inhibitors. *J. Med. Chem.* **2012**, *55*, 4457−4478.
(46) Kiselev, E.; Agama, K.; Pommier, Y.; Cushman, M. Azaindenoisoquinolines as Topoisomerase I Inhibitors and Potential Anticancer Agents: A Systematic Study of Structure-Activity Relationships. *J. Med. Chem.* **2012**, *55*, 1682−1697.
(47) Kiselev, E.; DeGuire, S.; Morrell, A.; Agama, K.; Dexheimer, T. S.; Pommier, Y.; Cushman, M. 7-Azaindenoisoquinolines as Topoisomerase I Inhibitors and Potential Anticancer Agents. *J. Med. Chem.* **2011**, *54*, 6106−6116.
(48) Kiselev, E.; Sooryakumar, D.; Agama, K.; Cushman, M.; Pommier, Y. Optimization of the Lactam Side Chain of 7-Azaindenoisoquinoline Topoisomerase I Inhibitors and Mechanism of Action Studies in Cancer Cells. *J. Med. Chem.* **2014**, *57*, 1289−1298.
(49) Nguyen, T. X.; Abdelmalak, M.; Marchand, C.; Agama, K.; Pommier, Y.; Cushman, M. Synthesis and Biological Evaluation of Nitrated 7-, 8-, 9-, and 10-Hydroxyindenoisoquinolines as Potential Dual Topoisomerase I (Top1)-Tyrosyl-DNA Phosphodiesterase I (TDP1) Inhibitors. *J. Med. Chem.* **2015**, *58*, 3188−3208.
(50) Davies, D. R.; Interthal, H.; Champoux, J. J.; Hol, W. G. J. Crystal Structure of a Transition State Mimic for Tdp1 Assembled from Vanadate, DNA, and a Topoisomerase I-derived Peptide. *Chem. Biol.* **2003**, *10*, 139−147.
(51) Schellenberg, M. J.; Appel, C. D.; Adhikari, S.; Robertson, P. D.; Ramsden, D. A.; Williams, R. S. Mechanism of Repair of 5′-Topoisomerase II-DNA Adducts by Mammalian Tyrosyl- DNA Phosphodiesterase 2. *Nat. Struct. Mol. Biol.* **2012**, *19*, 1363−1371.
(52) Hornyak, P.; Askwith, T.; Walker, S.; Komulainen, E.; Paradowski, M.; Pennicott, L. E.; Bartlett, E. J.; Brissett, N. C.;

DOI: 10.1021/acs.jmedchem.6b01565
J. Med. Chem. XXXX, XXX, XXX−XXX

Raoof, A.; Watson, M.; Jordan, A. M.; Ogilvie, D. J.; Ward, S. E.; Atack, J. R.; Pearl, L. H.; Caldecott, K. W.; Oliver, A. W. Mode of Action of DNA-Competitive Small Molecule Inhibitors of Tyrosyl DNA Phosphodiesterase 2. *Biochem. J.* **2016**, *473*, 1869−1879.
(53) Dexheimer, T. S.; Pommier, Y. DNA Cleavage Assay for the Identification of Topoisomerase I Inhibitors. *Nat. Protoc.* **2008**, *3*, 1736−1750.
(54) Antony, S.; Jayaraman, M.; Laco, G.; Kohlhagen, G.; Kohn, K. W.; Cushman, M.; Pommier, Y. Differential Induction of Topoisomerase I-DNA Cleavage Complexes by the Indenoisoquinoline MJ-III-65 (NSC 706744) and Camptothecin: Base Sequence Analysis and Activity against Camptothecin-Resistant Topoisomerase I. *Cancer Res.* **2003**, *63*, 7428−7435.
(55) Cushman, M.; Jayaraman, M.; Vroman, J. A.; Fukunaga, A. K.; Fox, B. M.; Kohlhagen, G.; Strumberg, D.; Pommier, Y. Synthesis of New Indeno[1,2-*c*]isoquinolines: Cytotoxic Non-Camptothecin Topoisomerase I Inhibitors. *J. Med. Chem.* **2000**, *43*, 3688−3698.
(56) Shoemaker, R. H. The NCI60 Human Tumour Cell Line Anticancer Drug screen. *Nat. Rev. Cancer* **2006**, *6*, 813−823.
(57) Bonner, W. M.; Redon, C. E.; Dickey, J. S.; Nakamura, A. J.; Sedelnikova, O. A.; Solier, S.; Pommier, Y. OPINION Gamma H2AX and Cancer. *Nat. Rev. Cancer* **2008**, *8*, 957−967.
(58) Redon, C. E.; Nakamura, A. J.; Sordet, O.; Dickey, J. S.; Gouliaeva, K.; Tabb, B.; Lawrence, S.; Kinders, R. J.; Bonner, W. M.; Sedelnikova, O. A. *gamma-H2AX Detection in Peripheral Blood Lymphocytes, Splenocytes, Bone Marrow, Xenografts, and Skin*; Springer: New York, 2011; Vol. *682*, pp 249−270.

DOI: 10.1021/acs.jmedchem.6b01565
J. Med. Chem. XXXX, XXX, XXX−XXX